

Constraints on the Origin of Chondrules and CAIs from Short-lived and Long-lived Radionuclides

N. T. Kita

*Department of Geology and Geophysics, University of Wisconsin-Madison, 1215
W. Dayton Street, Madison, WI 53706, USA*

G. R. Huss

*Hawai'i Institute of Geophysics and Planetology, University of Hawai'i at Manoa,
1680 East-West Road, Honolulu, HI 96822, USA*

S. Tachibana

*Department of Earth and Planetary Science, University of Tokyo, 7-3-1 Hongo,
Tokyo 113-0033, Japan*

Y. Amelin

*Geological Survey of Canada, 601 Booth Street, Rm. 693, Ottawa, ON, Canada
K1A 0E8*

L. E. Nyquist

*KR/NASA Johnson Space Center, 2101 NASA Parkway, Houston, TX 77058-3696,
USA*

I. D. Hutcheon

*Glenn T. Seaborg Institute, Lawrence Livermore National Laboratory, 7000 East
Ave., Livermore, CA 94551, USA*

Abstract. The chronology of the first few million years (My) of solar system history is reviewed based on high-precision absolute (Pb-Pb) and relative (short-lived radionuclide) age data. Pb-Pb ages indicate that calcium-aluminum-rich inclusions (CAIs), the oldest known solar system objects, formed 4567.2 ± 0.6 Ma ago. This is often referred to as the age of the solar system. Times of formation relative to the oldest CAIs for CAIs (≤ 0.3 My) and chondrules (1-3 My), and for early asteroidal differentiation (≥ 3 My) are comparable to time scales estimated from astronomical observations of low-mass young stars – protostars (class I), classical T Tauri stars (class II) and weak-

lined T Tauri stars (class III), respectively. The Pb-Pb ages of chondrules also indicate chondrule formation occurred within 1-3 My after CAIs. The ^{53}Mn - ^{53}Cr isochrons of bulk chondrules indicate chondrule formation contemporaneously with or within 2 My of CAI formation. Chondrules from different classes of chondrites show the same range of ^{26}Al ages in spite of having differences in oxygen isotopic compositions, indicating that chondrules formed in localized environments. A broad correlation between compositions and ^{26}Al - ^{26}Mg ages of chondrules in LL3 chondrites suggests elemental fractionation during chondrule formation.

1. Introduction

1.1. Radionuclides as Chronometers of the Early Solar System

One of the challenges of cosmochemistry is to understand the timing of events in the early solar system through the examination of tiny objects preserved in primitive meteorites. Many radionuclides with long half-lives ($t_{1/2} \geq 10^9$ years = Gy), called long-lived nuclides in geochronology (Table 1), have been applied to establish absolute ages of meteorites and their components (e.g., Patterson 1955; Tatsumoto, Knight, & Allègre 1973; Chen & Tilton 1976; Minster, Birck, & Allègre 1982). This earlier work gave ages of 4.5-4.6 Ga for various types of meteorites. However, the slow decay rate of these nuclides generally limits the time resolution to ≥ 20 My. Application of the meteorite age data to decipher the early evolution of the solar system is not easy because the time scales inferred from astronomical observations of young stars and from theoretical studies of planetary evolution are only of the order of ~ 10 My (e.g., Calvet, Hartmann, & Strom 2000). A time resolution of 1 My or less is thus necessary in order to distinguish the processes occurring at various evolutionary stages of a sun-like, low-mass star and a surrounding protoplanetary disk, such as protostars with high infall rates (≤ 0.1 My), classical T Tauri stars with dusty disks around central stars (≤ 3 My), and weak-lined T Tauri stars for which dusty disks are absent (indicating planetary evolution, ≤ 10 My).

Since the first observation of excess ^{129}Xe from the decay of ^{129}I (Jeffery & Reynolds 1961), the former existence of short-lived nuclides has been confirmed from the excesses of their daughter nuclides in meteorites. These nuclides, now extinct because of their short half-lives (≤ 100 My; Table 1), potentially provide chronometers with time resolution capable of distinguishing the small time differences between events in the earliest solar system. In this Chapter, we discuss the evidence for differences in the formation times of calcium-aluminum-rich inclusions (CAIs), chondrules, and other constituents in chondrites that formed in the protoplanetary disk during its short lifetime of ~ 3 My, which is typical for a disk surrounding a low-mass star (Calvet et al. 2000). The primary evidence comes from short-lived nuclides with half-lives less than 5 My, the most important of which are ^{26}Al , ^{53}Mn , and ^{60}Fe , as well as from the long-lived U-Pb system where high precision ^{207}Pb - ^{206}Pb ages are applied. These systems allow us to determine time differences of less than 1 My, short enough to elucidate the history of the protoplanetary disk. Other nuclides with

$t_{1/2} < 5$ My include ^{41}Ca and ^{36}S , which are limited to observations in CAIs (e.g., Srinivasan, Ulyanov, & Goswami 1994; Lin et al. 2004). Table 1 does not include ^{10}Be ($t_{1/2} = 1.5$ My), which is inferred to have been present in CAIs but is widely thought to have been produced by irradiation from solar energetic particles and may not be a useful chronometer (e.g., McKeegan, Chaussidon, & Robert 2000a; Marhus, Goswami, & Davis 2002; McPherson, Huss, & Davis 2003). The origins of the short-lived nuclides in the solar system are discussed in depth by Goswami et al. (this volume). Relative ages estimated from differences in initial $^{87}\text{Sr}/^{87}\text{Sr}$ ratios provide another approach to resolving the time differences of the order of 1 My. This technique has been applied to CAIs and some meteorites (Papanastassiou & Wasserburg 1969, Gray et al. 1973; Podosek et al. 1991). However, the method is strongly model-dependent and has rarely been used in recent studies, so we concentrate here on the short-lived radionuclides and Pb-Pb chronometry.

Table 1. Parent-daughter nuclide pairs used for meteorite chronology

Short-lived	$t_{1/2}$ My	Initial Solar Abundance	Long-lived	$t_{1/2}$ Gy [†]
^{41}Ca - ^{41}K	0.1	$^{41}\text{Ca}/^{40}\text{Ca}$ 1.4×10^{-8} [1]	^{40}K - ^{40}Ar	1.25
^{36}Cl - ^{36}S	0.3	$^{36}\text{Cl}/^{35}\text{Cl}$ $\geq 5.0 \times 10^{-6}$ [2]	^{87}Rb - ^{87}Sr	48.8
^{26}Al - ^{26}Mg	0.73	$^{26}\text{Al}/^{27}\text{Al}$ 5.0×10^{-5} [1]	^{147}Sm - ^{143}Nd	106
^{60}Fe - ^{60}Ni	1.5	$^{60}\text{Fe}/^{56}\text{Fe}$ $(0.5-1) \times 10^{-6}$ [3-5]	^{187}Re - ^{187}Os	41.6
^{53}Mn - ^{53}Cr	3.7	$^{53}\text{Mn}/^{55}\text{Mn}$ $\sim 9 \times 10^{-6}$ [6]	^{232}Th - ^{208}Pb	13.9
^{107}Pd - ^{107}Ag	6.5	$^{107}\text{Pd}/^{108}\text{Pd}$ 2×10^{-5} [1]	^{235}U - ^{207}Pb	0.704
^{182}Hf - ^{182}W	9	$^{182}\text{Hf}/^{180}\text{Hf}$ 1.0×10^{-4} [1]	^{238}U - ^{206}Pb	4.468
^{129}I - ^{129}Xe	16	$^{129}\text{I}/^{127}\text{I}$ 1.0×10^{-4} [1]		
^{244}Pu (fission)	80	$^{244}\text{Pu}/^{238}\text{U}$ 7.0×10^{-3} [1]		
^{146}Sm - ^{142}Nd	103	$^{146}\text{Sm}/^{144}\text{Sm}$ 8×10^{-3} [7]		

[1] McKeegan & Davis (2003), [2] Lin et al. (2004), [3] Huss & Tachibana (2004), [4] Mostefaoui, Lugmair, & Hoppe (2005), [5] Tachibana et al. (2005), [6] calculated from Lugmair & Shukolyukov (1998), Lugmair & Galer (1992), and Amelin et al. (2002), [7] Nyquist et al. (1994). [†]Data sources: Steiger & Jäger (1977) and Begemann et al. (2001).

1.2. Isochron Method

In principle, the age of an object, t , can be determined from the simple formula of radioactive decay, $P = P_0 \exp(-\lambda t)$, where P_0 and P are the abundance of the radioactive parent nuclide at the beginning and after time t , respectively, and λ is the decay constant, where λ is equal to $\ln(2)/t_{1/2}$. For long-lived-nuclide chronology, we measure the amounts of parent and radiogenic daughter nuclide in the sample today, P and D^* , where D^* is equal to $P_0 - P$, to obtain the “age t ”. Thus, the ratio between parent and daughter nuclides is expressed as a function of t as follows:

$$\frac{D^*}{P} = \exp(\lambda t) - 1 \quad (1)$$

In the case of a short-lived nuclide, the parent nuclide is now extinct and is no longer detectable in the samples, but the amount P at the time of formation is equal to the amount of radiogenic daughter nuclide D^* that is measured today. Here we define the isotopic ratio of a parent nuclide to a stable isotope of the same element, (P/P_S) .

If the solar system materials started with a homogeneous initial ratio for the short-lived nuclide with a value $(P/P_S)_0$, then the (P/P_S) is expressed by a relative time Δt since the formation of the solar system as follows,

$$\frac{P}{P_S} = \frac{D^*}{P_S} = \left(\frac{P}{P_S} \right)_0 \exp(-\lambda \Delta t) \quad (2)$$

Note that by definition the age t for a long-lived chronometer is counted backwards from the present to the past and is called the “absolute age”. In contrast, the relative age Δt for a short-lived chronometer is defined as time after “*time zero*”, and the relative age is counted forward from the past to the present. If we know $(P/P_S)_0$ of the newly born solar system, the relative ages Δt obtained for meteoritic components are directly comparable to the astronomical time scales of young stars that are determined by the spectra of central stars in the HR diagram (Calvet et al., 2000). However, even the oldest objects in meteorites, like CAIs, might not have formed exactly at the same time as the astronomically-defined birth of the solar system. For some nuclides, the best-determined isotopic ratios come from achondrites or iron meteorites that are obviously from asteroidal bodies formed significantly after the beginning of the solar system. Therefore, relative ages Δt are always given as the time before or after the formation of specific meteorite samples, such as “after CAIs” for ^{26}Al ages and “before LEW86010” angrite for the ^{53}Mn ages (see next section), and may have significant offsets when compared to astronomical time scales of the stellar evolution. The units used throughout this chapter are “Ma (Mega annum = 10^6 years)” and “Ga (Giga annum = 10^9 years)” for absolute ages and “My (million years = 10^6 years)” for relative ages.

The simple application of the radioactive decay equations Eq. (1-2) usually is not possible in practice. In many cases, the measured amount of the daughter nuclide (D) consists of both radiogenic (D^*) and nonradiogenic (D_0) components. The latter is initially contained in the samples at the time of crystallization. Therefore, Eq. (1) and (2) are usually replaced with a formula consisting of measurable properties,

$$\frac{D}{D_S} = \frac{D_0}{D_S} + \frac{P}{D_S} [\exp(\lambda t) - 1] \quad \text{for a long-lived nuclide (1'),}$$

$$\frac{D}{D_S} = \frac{D_0}{D_S} + \frac{P_S}{D_S} \left(\frac{P}{P_S} \right)_0 \exp(-\lambda \Delta t) \quad \text{for a short-lived nuclide (2'),}$$

where D_S is a stable isotope of the daughter nuclide. Both equations are expressed as linear formulae between D/D_S and P/D_S (or P_S/D_S). By obtaining several measurements with different parent to daughter ratios and plotting the data on an isochron diagram (Fig. 1), the age of a sample can be determined from the slope of the linear regression, and the intercept with the y-axis gives the initial isotopic ratio for daughter nuclide prior to the addition of decay products.

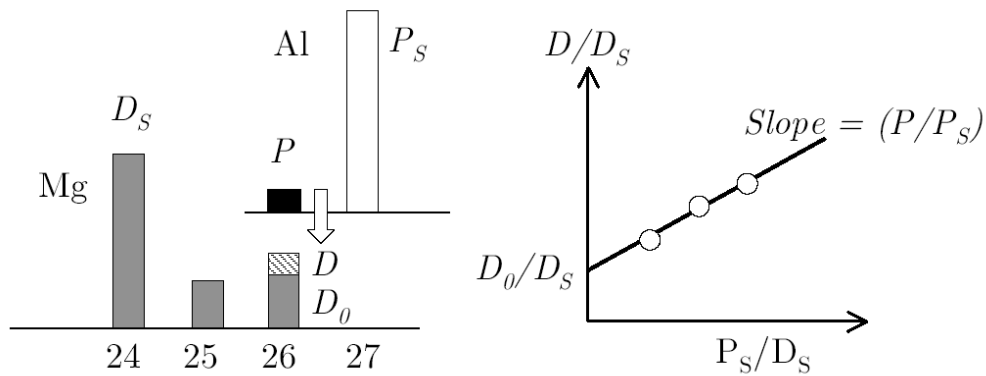


Figure 1. Example of an isochron diagram for ^{26}Al decay to ^{26}Mg . The isotopic ratio of the short-lived nuclide to its stable isotope (P/P_S) is determined from the best-fit line (called an “isochron”) for a set of data from a single sample that have a range of (P_S/D_S) ratios. The slope of the isochron, (P/P_S), changes exponentially with time according to Eq. (2) thus defining the sample’s age.

Obviously, multiple measurements are required to obtain a single age. The measurements can be from a set of several bulk CAIs or chondrules, a set of mineral separates from a rock or meteorite, or one can make *in situ* measurements of different mineral phases (such as pyroxene and plagioclase) in single CAI or chondrule. An isochron age based on the regression of a set of samples is valid only if three criteria are met. First, the studied “set of samples” must have formed simultaneously. Second, these samples must have had identical D_0/D_S and P/P_S , at the time of formation. Third, the “system” (the entire set of objects being dated) must have remained closed to the migration of parent and daughter isotopes since the event that is being dated. Variations in parent-daughter elemental ratios P/D_S , produced by chemical fractionation during formation of the objects, are a prerequisite of isochron dating. Chemical fractionation and isotopic homogenization can occur during melting and subsequent crystallization or during evaporation and subsequent condensation of minerals from a gas. None of the chondritic meteorites containing CAIs and chondrules have entirely avoided secondary processing in their parent bodies, even the lowest petrologic subtypes (e.g., Alexander, Barber & Hutchison 1989; Grossman & Brearley 2005). Later diffusion of isotopes and chemical reactions among the phases may disturb the isochron dating the primary event. The advantage of the isochron method is that well-defined isochrons certify that secondary processes have not affected the isotope system used for dating and assure that the data have chronological significance. In practice, the challenge is to show that the isochron is well defined.

Even when these criteria are met for individual samples and the initial abundance of the parent nuclide in the sample is correctly deduced, the time interval between the formation of two objects, obtained from Eq. (2') is based on the assumption of an initially homogeneous distribution of radioactive nuclides in the solar nebula where these objects formed. A short-lived nuclide in the solar nebula could be het-

erogeneously distributed if materials from stellar sources with a variety of isotopic ratios were not well mixed. Some of the radionuclides might also have been locally produced, for example, by energetic particles (see Goswami et al. and Gounelle & Russell, this volume). As a result, the estimated (P/P_S) may not be only a function of Δt as given in Eq. (2). The assumption of isotopic homogeneity can be tested by comparing the ages obtained from several chronometers. As will be discussed later, the Pb-Pb, ^{26}Al and ^{53}Mn ages are generally, if not completely, consistent, which implies at least first-order homogeneity of ^{26}Al and ^{53}Mn in the solar system. In contrast, initial $^{10}\text{Be}/^9\text{Be}$ and $^{26}\text{Al}/^{27}\text{Al}$ ratios in CAIs are found to be inconsistent (e.g., McKeegan et al. 2000a; MacPherson et al. 2003), supporting the local production model for ^{10}Be in the solar system (see Goswami et al., this volume). Thus, the search for agreement among short-lived chronometers is a main theme of age-determination studies.

Isotope-ratio mass spectrometers used for determination of isotopic ratios in early solar system materials utilize three different ionization techniques: thermal ionization (TIMS), inductively coupled plasma (ICP-MS), and secondary ion emission induced by a primary ion beam (SIMS, or ion microprobe). The first two techniques are more suitable for high precision isotopic analyses (0.001-0.1%), whereas the strength of SIMS is high spatial resolution, up to μm -scale. SIMS is therefore best suited for *in situ* analysis of the small individual mineral grains in chondrules and CAIs.

1.3. Elemental Fractionation between Parent and Daughter Nuclides

In the protoplanetary disk, evaporation and condensation played an important role in homogenizing the isotopes by passing them through the gas phase. In the classical model for the major chemical fractionations among chondrite classes, solids condensed from a hot gaseous nebula of solar composition (e.g., Grossman & Larimer 1974). Even if the classical model is incorrect and all solids were not evaporated on a nebula-wide scale, local evaporation and recondensation would have played a similar role. The 50% condensation temperature (T_C) is the temperature at which half of the abundance of a given element is present as a solid (e.g., Lodders 2003), and is a useful parameter for comparing the volatility of various elements (Fig. 2a). Within individual CAIs and chondrules, igneous fractionation occurred internally during melting and crystallization. Experimentally determined mineral/melt partition coefficients (Fig. 2b) are useful for describing differences in element partitioning among minerals within chondrules and igneous CAIs. The bulk compositions of chondrules and CAIs and the distribution of elements within them result from a superposition of volatility-related and igneous fractionations.

Aluminum and U are *ultrarefractory* elements ($T_C > 1650\text{K}$) that are significantly enriched in CAIs. Their radioactive isotopes (^{26}Al , ^{235}U , ^{238}U) decay to isotopes of Mg and Pb, elements that have much lower condensation temperatures ($T_C \sim 1300\text{K}$ and $T_C = 727\text{K}$, respectively). Thus, radiogenic Mg and Pb isotopic compositions in bulk CAIs reflect the chemical fractionation associated with the event(s) that isolated the CAIs from bulk solar system material. To the extent that a suite of samples falls on a single isochron in the Al/Mg system or give the same ages by Pb-Pb dating, the chemical fractionation could have been a single event or a series of events

occurred too close together to be resolved by the measurements. This might have been nebular condensation, which is a clearly defined event, or it may reflect a vaporization event that enriched residual solids in refractory elements, followed by the CAI melting event. A key challenge for future workers is to determine what event(s) may be represented by so-called “whole rock” ages.

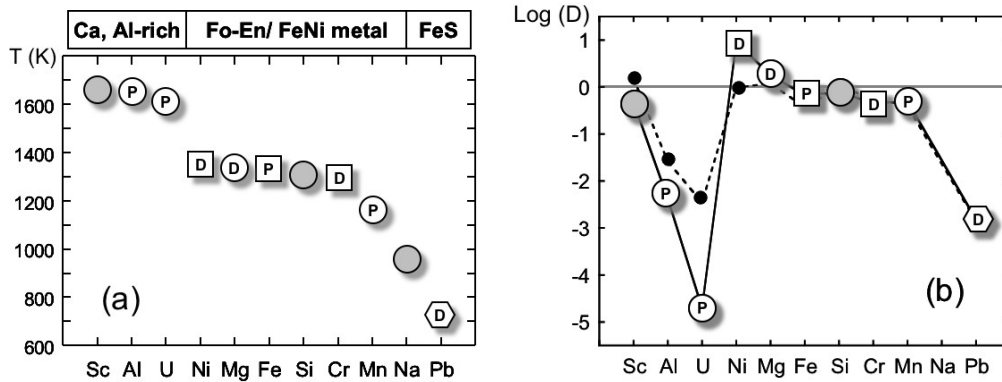


Figure 2. Chemical fractionation among parent/daughter nuclide pairs. “P” indicates parent nuclides, “D” daughter nuclides, and others (grey) reference elements. (a) The 50% condensation temperatures in the solar nebular ($P = 10^{-4}$ atm, after Lodders 2003). Circles, squares and hexagons indicate lithophile (condensed as oxide and silicates), siderophile (metals), and chalcophile (sulfide) elements. (b) Experimental mineral/melt distribution coefficients (Kennedy et al. 1993). Solid line, olivine ($T = 1525^{\circ}\text{C}$); dashed line, orthopyroxene ($T = 1440^{\circ}\text{C}$). Values for Sr are used as an approximation for Pb. The same symbols are used as in (a) though metal and sulfide phases are absent from the system. Residual melts and plagioclase crystallized from CAIs and chondrule melts all have high Al/Mg ratios.

The other type of age measured for the Al-Mg system comes from internal isochrons. Chondrules and some CAIs crystallized from melts and the Al and Mg were partitioned among the constituent minerals, such as anorthite ($\text{CaAl}_2\text{Si}_3\text{O}_8$), melilite ($\text{Ca}_2[\text{Mg,Al}][\text{Si,Al}]_2\text{O}_7$), spinel (MgAl_2O_4), and pyroxene in CAIs and olivine, pyroxene, plagioclase and glass in chondrules. If the system is undisturbed, excesses of ^{26}Mg will correlate with the Al/Mg ratio of individual phases (Fig. 1). In such cases, the ages correspond to the melting events.

Iron and Mn are less refractory than Al and U, and thus they are present in CAIs in only low abundances, often largely in secondary minerals. Therefore, the Fe-Ni and Mn-Cr systems are less suitable for dating CAIs. Iron and Ni have nearly identical condensation temperatures ($T_C = 1334\text{K}$ and 1353K , respectively) and thus do not fractionate significantly via volatility-driven processes. However, large fractionations can be produced under oxidizing conditions because Fe is more easily oxidized than Ni and preferentially goes into oxides and silicates. Minerals with very high Fe/Ni ratios include olivine, pyroxene, magnetite, and sulfides. Enhancements of ^{60}Ni that correlate with the Fe/Ni ratio recently have been observed in pyroxene,

magnetite, and sulfides (Tachibana & Huss, 2003; Mostefaoui et al. 2003; Huss & Tachibana 2004; Mostefaoui, Lugmair, & Hoppe 2004, Mostefaoui et al. 2005; Tachibana et al. 2005). In order for these new data to provide chronological information, the measured minerals must have remained in closed systems since they formed. This is a key issue of contention for the Fe-Ni system.

There is a modest difference in the condensation temperatures of Mn and Cr ($T_C = 1158\text{K}$ and 1296K respectively). This results in only a limited range of Mn/Cr fractionation among chondritic materials. However, a small amount of Cr condenses into spinel at high temperatures ($\sim 1800\text{K}$, Ebel & Grossman 2000) and into metal and Mg silicate at moderate temperatures ($\sim 1300\text{K}$). This might cause significant depletions of Mn relative to Cr in high temperature condensates. An example is spinel in CAIs, which shows low Mn/Cr ratios that help to provide the spread in an isochron diagram (e.g., Birck & Allègre 1985). Another application of the ^{53}Mn - ^{53}Cr chronometer is for chondrules, which show significant variation in their bulk Mn/Cr ratios. If the early high temperature condensates were incorporated into chondrule precursors and the bulk Mn/Cr ratios were preserved during chondrule-forming events (closed system formation), the ^{53}Mn - ^{53}Cr isochron of bulk chondrules would provide the time of nebular Mn/Cr fractionation. However, because Mn and Cr are both more volatile than Mg, the Mn-Cr system may not have been closed during chondrule formation. The extent to which chronological information has been retained in bulk ^{53}Mn - ^{53}Cr isochrons of chondrules is a question open to examination.

2. Age Determinations of CAIs and Chondrules

2.1. ^{207}Pb - ^{206}Pb System

Short-lived chronometers have become the main tools for studying the chronology of early solar system processes, despite the fact they can only measure time intervals. In order to link relative ages based on short-lived chronometers to the absolute time scale, we must use high precision Pb isotopic dates from the same meteorite components. High precision and accuracy of Pb isotopic dates for chondrules and CAIs are, therefore, crucial for building a comprehensive isotopic timescale of the early solar system. The U-Pb dating method (Faure 1986; Dickin 1995) includes two isotopes of uranium that decay into two different isotopes of lead at different rates (Table 1). This dual decay scheme allows an age to be calculated from the ratio of the radiogenic isotopes $^{207}\text{Pb}^*$ and $^{206}\text{Pb}^*$ alone, without using U/Pb ratios. Combining Eq. (1') for two U-Pb decay systems gives the Pb-Pb isochron equation as follows:

$$\frac{\left(\frac{^{207}\text{Pb}}{^{204}\text{Pb}}\right) - \left(\frac{^{207}\text{Pb}}{^{204}\text{Pb}}\right)_0}{\left(\frac{^{206}\text{Pb}}{^{204}\text{Pb}}\right) - \left(\frac{^{206}\text{Pb}}{^{204}\text{Pb}}\right)_0} = \left(\frac{^{235}\text{U}}{^{238}\text{U}}\right) \frac{\exp(\lambda_{235}t) - 1}{\exp(\lambda_{238}t) - 1} \quad (3)$$

The left side of the above formula is equal to the radiogenic Pb isotopic ratio ($^{207}\text{Pb}^*/^{206}\text{Pb}^*$), so that the age t is obtained without knowledge of parent/daughter ratios:

$$\frac{{}^{207}\text{Pb}^*}{{}^{206}\text{Pb}^*} = \frac{{}^{235}\text{U} \exp(\lambda_{235}t) - 1}{{}^{238}\text{U} \exp(\lambda_{238}t) - 1} = \frac{1}{137.88} \frac{\exp(\lambda_{235}t) - 1}{\exp(\lambda_{238}t) - 1} \quad (4)$$

The ${}^{207}\text{Pb}^*/{}^{206}\text{Pb}^*$ ratio and, hence, the age is determined from a Pb-Pb isochron, a plot of measured ${}^{207}\text{Pb}/{}^{206}\text{Pb}$ ratios versus ${}^{204}\text{Pb}/{}^{206}\text{Pb}$ for a set of samples (as in Fig. 3). As shown in Eq. (3), ${}^{204}\text{Pb}$ is the nonradiogenic stable isotope and is, therefore, used as a gauge of the amount of Pb present in the object at the time of formation (called “initial Pb”). The intercept of the isochron with the Y-axis gives the ${}^{207}\text{Pb}^*/{}^{206}\text{Pb}^*$ ratio of Eq. (4), which corresponds to the time of the event that caused parent-daughter elemental fractionation.

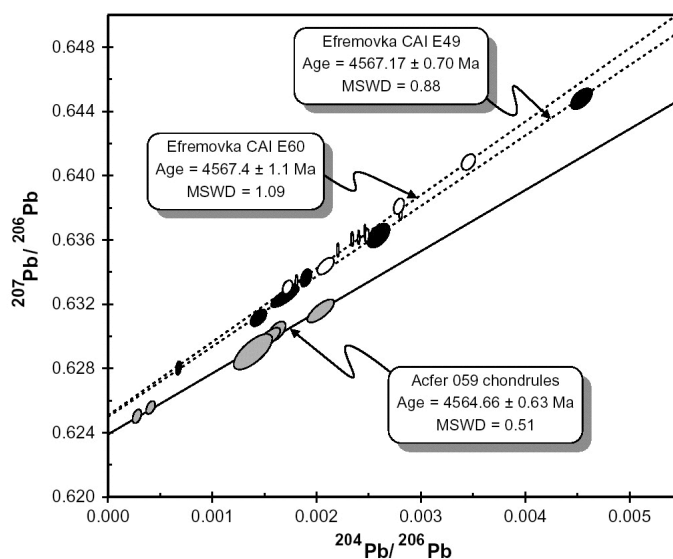


Figure 3. Pb-Pb isochrons for chondrules and CAIs (Amelin et al. 2002).

The ${}^{207}\text{Pb}^*/{}^{206}\text{Pb}^*$ method is unique among isotopic chronometers in two ways. First, since the date is determined from the ratio of isotopes for one element, it is insensitive to recent fractionation between U and Pb, caused either by natural processes, e.g., recent impact or terrestrial weathering, or induced by laboratory treatment, e.g., partial dissolution. Second, the relatively short half-life of ${}^{235}\text{U}$ (0.7 Gy) results in rapid growth of radiogenic ${}^{207}\text{Pb}^*/{}^{206}\text{Pb}^*$, allowing small age differences (0.5-1 My) to be resolved. This precision approaches the precision of state-of-the-art, short-lived-nuclide dating techniques. Because of its high time resolution, the ${}^{207}\text{Pb}^*/{}^{206}\text{Pb}^*$ method is the only way to obtain “absolute” ages suitable for studies of solar nebula evolution. Thus, this is also the only method used for linking extinct-nuclide chronometers to the absolute timescale (see Amelin 2005 for a more-detailed discussion).

The Pb-Pb method was the first chronometer used to date meteorites (Patterson 1955, 1956), and many data had been obtained by the early 1980's (see reviews by Tilton 1988a, b). Earlier work on CAIs done by Tatsumoto, Unruh & Desborough (1976), Chen & Tilton (1976) and Chen & Wasserburg (1981) indicated old ages of 4.55-4.57 Ga. More recently, Allègre, Manhès, & Göpel (1995) obtained an average Pb-Pb age for CAIs of 4566 ± 2 Ma. They recognized a tendency that the model Pb-Pb ages of individual CAIs increase with measured radiogenic Pb isotope ratios ($^{206}\text{Pb}/^{204}\text{Pb}$). This may be caused by inadequate correction for initial Pb. At the same time, an acid-leaching technique to remove contamination from terrestrial Pb and Pb of unknown origin (called as "common Pb" including initial Pb in the sample) was proven useful in obtaining high precision Pb-Pb ages from meteorites (Lugmair & Galer, 1992; Göpel, Manhès, & Allègre 1994). Amelin et al. (2002) obtained high-precision Pb-Pb ages for two CAIs from Efremovka (CV3) and for a group of chondrules from Acfer 059 (CR), as shown in Figure 3. The result indicated the time difference between formation of CAIs (4567.2 ± 0.7 Ma) and chondrules (4564.7 ± 0.6 Ma) was 2.5 ± 1.2 My, consistent with the ~ 2 My difference inferred from the Al-Mg systems (e.g., Russell et al. 1996; Kita et al. 2000; Huss et al. 2001). A subsequent study of chondrules from Allende (CV3) showed Pb-Pb age of 4566.7 ± 1.0 Ma (Amelin et al. 2004). These data imply that chondrule formation in the nebular setting started simultaneously with or shortly after CAI formation and continued for at least 2 My.

It should be mentioned, however, that the Pb-Pb age is only meaningful if the parent-daughter system remained closed since its formation, or if the disturbance was so recent that its radiogenic Pb-isotopic ratios were not affected. The leaching technique may cause selective leaching between U and Pb and result in biased absolute ^{238}U - ^{206}Pb ages. For these samples, it is not possible to evaluate whether the U-Pb system had remained closed. However, high precision Pb-Pb ages obtained after acid leaching have several advantages over obtaining accurate $^{238}\text{U}/^{206}\text{Pb}$ ratios, which only provide ages with lower time resolution (>10 My). Complete removal of common Pb from chondrules and CAIs prior to Pb isotopic analyses is the only efficient solution for problems caused by the presence of multiple common-Pb components (Amelin 2005; Amelin et al. 2002; Amelin, Ghosh, & Rotenberg 2005). It is only possible to reliably recognize open-system behavior of radiogenic Pb and multistage evolution of the U-Pb system (for example, incorporation of radiogenic Pb that was accumulated in a chondrule or CAI precursor) if common Pb is absent (Amelin 2005). Elimination of common Pb is, therefore, the most important condition for precise and accurate Pb isotopic dating.

The best solution for resolving small differences in age within a single population of CAIs or chondrules would be to construct internal isochrons by analysis of multiple fragments from the same chondrule or CAI. However, the usefulness of this approach is restricted by the small sizes of most chondrules and CAIs and the low abundance of U and radiogenic Pb in their constituent phases. A typical 1 mm chondrule (ca. 1.5 mg in weight) may contain only 15 pg and 9 pg of radiogenic ^{206}Pb and ^{207}Pb , respectively. Extensive acid washing, necessary for removal of common Pb, further reduces the content of radiogenic Pb to 20-30% of the original amount. These amounts are at the limit of modern techniques for precise Pb isotopic analysis. Sub-milligram fragments of chondrules contain insufficient radiogenic Pb to yield useful

precision. Internal-isochron Pb-Pb dating is therefore problematical for typical chondrules, but may be possible for exceptionally large chondrules with diameters of 3 mm or larger, and for large CAIs from CV chondrites.

The Pb-Pb ages of chondrules in the CB_a chondrite Gujba (4562.7±0.5 Ma) and in the CB_b chondrite Hammadah al Hamra 237 (4562.8±0.9 Ma) (Krot et al. 2005a) are the youngest precise absolute ages of chondrules determined from unequilibrated chondrites and are distinctly younger than the ages of chondrules in CR and CV chondrites (Amelin et al. 2002; 2004). The very-metal-rich CB chondrites are thought to have formed from metal and silicate droplets by evaporation and/or condensation in an impact-generated vapor plume (Rubin et al. 2003). In this scenario, the formation of CB chondrites was not a nebular process, and the ages of chondrules in CB chondrites do not provide a constraint on the lifespan of the nebula. If the data for CB chondrules are excluded, then the ages of CR-chondrite chondrules and CV-chondrite CAIs and chondrules discussed above would seem to constrain the lifetime of the nebula to about 2-3 My.

2.2. ²⁶Al-²⁶Mg System

²⁶Al has a half-life of 0.73 My, making it suitable to investigate the earliest stages of solar system history. Since the earliest observations of excess, radiogenic ²⁶Mg in CAIs from the Allende meteorite (Gray & Compston 1974; Lee & Papanastassiou 1974), large numbers of CAIs have been studied, yielding unambiguous evidence for the former existence of live-²⁶Al in the solar system with an initial ²⁶Al/²⁷Al ratio of ~5×10⁻⁵ (e.g., Lee, Papanastassiou, & Wasserburg 1976). MacPherson, Davis, & Zinner (1995) summarized the available data collected prior to 1995 and reached three important conclusions: (1) the distribution of inferred initial ²⁶Al/²⁷Al ratios is bimodal with most CAIs showing initial ²⁶Al/²⁷Al ratios of ~5×10⁻⁵, often referred as the “canonical value” for the solar system; (2) no CAIs formed with ²⁶Al/²⁷Al ratios significantly greater than 5×10⁻⁵; and (3) many CAIs experienced secondary metamorphism leading to Mg-isotope equilibration and lower inferred initial ²⁶Al/²⁷Al ratios. An important advance after the review by MacPherson et al. (1995) was the addition of new data for CAIs and chondrules from a diverse suite of unequilibrated carbonaceous and ordinary chondrites and for some achondritic plagioclase (see also a review by McKeegan & Davis 2003). Many of these data were obtained by new instrumentation and techniques developed during the last decade, including high-precision, large-radius SIMS, and multi-collector ICP-MS (MC-ICPMS) using both chemical processing and laser ablation. Recent measurements suggest that the initial ²⁶Al/²⁷Al ratio in the solar system was 25 – 30% higher than the canonical 5 × 10⁻⁵ value (Galy, Hutcheon, & Grossman 2004; Young et al. 2005; Taylor et al. 2004; Taylor, McKeegan, & Krot 2005). These new data sometimes appear to be in conflict with existing TIMS and SIMS data, and these discrepancies are currently the subject of considerable debate (e.g., Davis et al. 2005; Young et al. 2005).

The use of the ²⁶Al-²⁶Mg system as a chronometer is predicated on the assumption that the initial ²⁶Al/²⁷Al ratio was homogeneous throughout the nebula, and hence that the diverse solids produced from the nebula have isotopic differences that relate only to chronology and not to isotopic heterogeneity. With this assumption,

^{26}Al - ^{26}Mg ages can be calculated relative to the time that the $^{26}\text{Al}/^{27}\text{Al}$ ratio of the solar system was equal to the canonical value:

$$\Delta t = \frac{1}{\lambda_{26}} \ln \left\{ \left(\frac{^{26}\text{Al}}{^{27}\text{Al}} \right)_{\text{CAI}} / \left(\frac{^{26}\text{Al}}{^{27}\text{Al}} \right)_{\text{Sample}} \right\} \quad (5),$$

where λ_{26} is the decay constant of ^{26}Al . In the following discussion we assume a homogeneous distribution of ^{26}Al and express differences in inferred initial $^{26}\text{Al}/^{27}\text{Al}$ in terms of age relative to CAI formation.

2.2.1. Range of Initial $^{26}\text{Al}/^{27}\text{Al}$ Ratios in CAIs

Large numbers of CAIs from C chondrites (CV, CO, CH, CM, and CR) have been measured for the ^{26}Al - ^{26}Mg system, and the initial $^{26}\text{Al}/^{27}\text{Al}$ of most CAIs falls between 4×10^{-5} and 5×10^{-5} , corresponding to time differences of less than 0.3 My (data summarized by Wadhwa & Russell 2000; McKeegan & Davis 2003). Although other groups of chondrites contain few CAIs (<0.1%), CAIs in LL3 and EH3 chondrites showed initial $^{26}\text{Al}/^{27}\text{Al}$ ratios consistent with the canonical value of 5×10^{-5} within analytical uncertainties (Russell et al. 1996; Guan et al. 2000; Huss et al. 2001). Bizzarro, Baker, & Haack (2004) reported high precision ICP-MS data of six micro-drilled Allende CAIs, which fall on a well-defined isochron with a slope corresponding to $(^{26}\text{Al}/^{27}\text{Al}) = (5.25 \pm 0.10) \times 10^{-5}$, and appear to confirm previous results. However, data from bulk analyses of CAIs, together with Laser Ablation ICP-MS and SIMS analyses of minerals in CAIs plot significantly above the canonical isochron and imply “supracanonical $^{26}\text{Al}/^{27}\text{Al}$ ratios” of $(6-7) \times 10^{-5}$ (Galy et al. 2000; 2004; Taylor et al. 2004; 2005; Young et al. 2005). Interpretation of the supracanonical ratio is still an unresolved issue. Podosek et al. (1991) interpreted similar data in terms of later disturbance of the Al-Mg isotopic systematics, where radiogenic ^{26}Mg in anorthite was redistributed into melilite. Davis et al. (2005) pointed out that artificial ^{26}Mg excesses could be produced by using the wrong law to correct for mass fractionation. This is important because CAIs are enriched in heavy Mg isotopes significantly (5-10‰/amu), and because the ICPMS technique has a large, but well determined, instrumental mass fractionation. However, careful evaluation has shown that incorrect mass fractionation laws cannot explain all data that plot above the canonical isochron. Alternatively, Young et al. (2005) consider CAIs formed with the supracanonical ratios, and Al and Mg redistributed within each CAI by repeated high temperature thermal events (resetting the internal isochrons) during their 0.3 My residence in the protoplanetary disk. Although there is an inconsistency between these supra-canonical isochrons and the well-defined isochron by Bizzarro et al. (2004), these data suggest the solar system initial $^{26}\text{Al}/^{27}\text{Al}$ ratio was at least 25% higher than the canonical value and that the lower value commonly measured in CAIs reflects continued processing in the nebula over an interval of ~ 0.3 My. More investigations are required to determine if the initial abundance of ^{26}Al was substantially higher than has been assumed for nearly 30 years and to explore the possible implications for the thermal history of CAIs in the solar nebula.

MacPherson et al. (1995) pointed out that significant numbers of CAIs have ^{26}Al - ^{26}Mg isotopic compositions lying off the reference isochron, implying that the ^{26}Al - ^{26}Mg isotopic systems were locally disturbed by secondary events, occurring

over several My. Many CAIs have experienced complex thermal histories, either by reprocessing in the nebula or by being metamorphosed in parent bodies. Hsu, Wasserburg, & Huss (2000) showed that petrologically distinct units within Allende CAI 5241 have distinct initial $^{26}\text{Al}/^{27}\text{Al}$ ratios. The oldest unit has a canonical $^{26}\text{Al}/^{27}\text{Al}$ ratio, and other units given lower ratios corresponding to relative age differences of 0.1 My and 0.4 My. This result strongly suggests that there were sequential nebular heating events affecting some CAIs extending over a time scale of a few times 10^5 years. There are also a number of CAIs exhibiting disturbance in ^{26}Al - ^{26}Mg data in which some part of the inclusion contains the canonical $^{26}\text{Al}/^{27}\text{Al}$ ratios while other parts display much lower initial $^{26}\text{Al}/^{27}\text{Al}$ ratios (Hutcheon 1982a; Podosek et al. 1991; MacPherson & Davis 1993; Caillet, MacPherson, & Zinner 1993; Imai & Yurimoto 2000; Kita et al. 2004). Anorthite, the phase with highest Al/Mg ratio in most CAIs, is a particularly bad actor, often showing very little or no resolvable excess radiogenic $^{26}\text{Mg}^*$ in spite of very high $^{27}\text{Al}/^{24}\text{Mg}$ ratios (>100). These disturbed data are generally interpreted in terms of secondary, metamorphic events, taking place after ^{26}Al had decayed, several My after CAI crystallization.

Insofar as the isotopic disturbance of the ^{26}Al - ^{26}Mg system is controlled by Mg diffusion within and among coexisting CAI minerals, the different diffusivities for Mg can be used to place limits on the temperature and time of metamorphism. LaTourrette & Wasserburg (1998) measured Mg self-diffusion in anorthite and concluded that temperatures extant during parent body metamorphism were too low for Mg diffusion to play a dominant role for Allende and other C chondrites. However, both LaTourrette & Hutcheon (1999) and Yurimoto et al. (2000) demonstrated that coupled Mg diffusion between melilite and anorthite could explain the disturbed Mg isotope systematics in many Type B CAIs. Processes other than solid-state diffusion may also play a role. There is ample evidence of parent body metamorphism and fluid transport in many C chondrites. Reactions such as the replacement of anorthite by nepheline ($[\text{Na},\text{K}]\text{AlSiO}_4$) require open system behavior and suggest the Mg isotope record of CAIs reflects the influence of a variety of metamorphic processes. One of the challenges of future research will be to use isotope data to constrain metamorphic history and to distinguish between open- and closed-system processes.

There are minor groups of CAIs, particularly many of the hibonite (CaAl_2O_7)- and grossite (CaAl_4O_7)-bearing CAIs in CM and CH chondrites, which show only very small or unresolved ^{26}Mg excesses (MacPherson et al. 1995; Weber, Zinner, & Bischoff 1995). Some of them systematically contain significant isotopic anomalies in other elements, especially Ca and Ti (e.g., Ireland, Fahey, & Zinner 1988). Included in this group are CAIs exhibiting large mass-dependent isotopic fractionation of oxygen, Mg and Si, the so-called FUN inclusions (so-named because they exhibit Fractionation and Unidentified Nuclear effects). Because of the large nuclear isotope anomalies and highly refractory chemical compositions, these CAIs are most plausibly considered to have originated from isotopically heterogeneous region of the nebula that was missing the ^{26}Al characteristic of “normal” solar system material. Whether this lack of ^{26}Al is due to very early formation, before a “late” ^{26}Al addition from a stellar source, or to a more pervasive ^{26}Al heterogeneity in the nebula is a key issue for the utility of the ^{26}Al - ^{26}Mg chronometer for deciphering early solar system history.

2.2.2. Variation of Initial $^{26}\text{Al}/^{27}\text{Al}$ Ratios among CAI Types

Major element compositions and mineral compositions of CAIs indicate that the varieties of CAIs might be related to condensation sequences, starting from ultrarefractory hibonite- and grossite-bearing inclusions, Type A, to Type B, and then to less refractory Type C and FoB (forsterite bearing Type B) CAIs. There are no significant differences between the highest $^{26}\text{Al}/^{27}\text{Al}$ ratios among different CAI types, indicating that all of these CAIs formed in a time period shorter than the time resolution of ^{26}Al - ^{26}Mg dating (≤ 0.1 My). However, most Type C CAIs show much lower initial $^{26}\text{Al}/^{27}\text{Al}$ than the canonical value ($< 6 \times 10^{-6}$; Hutcheon 1982b; Krot et al. 2005b), indicating that these less refractory inclusions formed at least 2 My after Type A and B CAIs. These Type C CAIs often contain relic chondrule fragments and are ^{16}O poor, leading Krot et al. to suggest they were remelted during a chondrule formation episode ~ 2 My after formation of most CAIs. Other Type C CAIs (Imai & Yurimoto 2000; Kita et al. 2004) contain pyroxene and melilite plotting along the canonical ^{26}Al - ^{26}Mg isochron, indicating that at least some Type C CAI formed at the same time as Type A and B CAIs. These Type C CAIs may contain anorthite showing little or no ^{26}Mg excess, consistent with a later reheating event.

Amoeboid olivine aggregates (AOAs) are much less refractory than Type A and B CAIs, showing compositions intermediate between CAIs and chondrules. Itoh et al. (2002) reported initial $^{26}\text{Al}/^{27}\text{Al}$ ratios $\sim 3 \times 10^{-5}$, corresponding to ages 0.5 My younger than CAIs. Plagioclase-olivine inclusions (POIs) span a wide range in chemical composition, falling between ferromagnesian chondrules and fine-grained spinel-rich CAIs (Sheng 1992; Sheng, Hutcheon, & Wasserburg 1991; 1992). More recent work considers POIs to be a subset of Al-rich chondrules (e.g., Krot, Hutcheon, & Keil 2002; MacPherson & Huss 2003). POIs define isochrons with initial $^{26}\text{Al}/^{27}\text{Al}$ ratios less than 10^{-5} (Sheng et al. 1991; Hsu, Wasserburg, & Huss 2003; Kita et al. 2004), a behavior similar to chondrules. Together with increasing numbers of chondrule data described below, these results from the ^{26}Al - ^{26}Mg chronometer give us some hints of the overall sequence of material forming in the solar system, with CAIs forming first, followed by AOAs, and then POIs and chondrules (Fig. 4).

2.2.3. Chondrules

Chondrules usually do not contain Al-rich minerals with high Al/Mg ratios, making it difficult to investigate their initial $^{26}\text{Al}/^{27}\text{Al}$ ratios. Small numbers of Al-rich chondrules ($\leq 1\%$) with a wide variety of texture and compositions are present in most chondrite classes (Bischoff & Keil 1984; Krot & Keil 2002). These chondrules contain plagioclase and/or glass with high Al/Mg, and are potential targets for ^{26}Al chronology. The first detection of radiogenic ^{26}Mg in an ordinary chondrite was not from an Al-rich chondrule, but from the “clast chondrule” CC1 in Semarkona (LL3.0), a nonporphyritic, plagioclase-bearing chondrule, showing an initial $^{26}\text{Al}/^{27}\text{Al}$ ratio of $(7.7 \pm 2.1) \times 10^{-6}$ (Hutcheon & Hutchison 1989). Based on the high and strongly fractionated REE contents in plagioclase and pyroxene, CC1 was considered to be a fragment of an igneous rock set into the chondritic host. In this model the ^{26}Al - ^{26}Mg age of CC1 indicates that igneous activity was occurring on the asteroidal body at ~ 2 My after CAI formation. Later studies on similar chondrules indicate that non-porphyritic, anorthite-bearing chondrules are a minor type of FeO-rich and al-

kali-poor chondrule in UOCs, based on their chondritic bulk chemical compositions and high MgO contents ($\sim 0.5\%$) in anorthite (Kita et al. 2000; Mostefaoui et al. 2002; Tachibana et al. 2003). Trace-element data have not been collected on the majority of these anorthite-bearing, FeO-rich chondrules, so it is unclear whether or not they were all derived from asteroidal bodies. However, the ^{26}Al - ^{26}Mg record clearly indicates that these plagioclase bearing chondrules formed within ~ 2 My of CAIs.

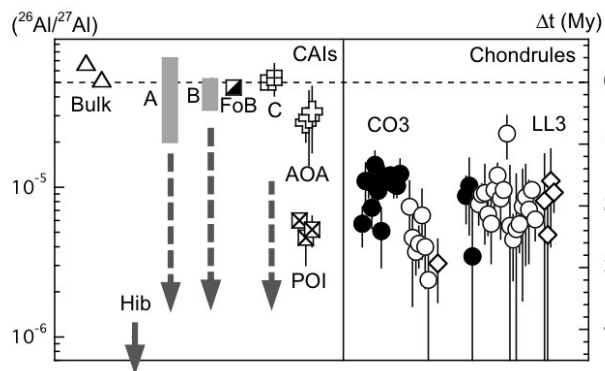


Figure 4. Initial $^{26}\text{Al}/^{27}\text{Al}$ ratios of CAIs and chondrules. Bulk CAIs: Galy et al. (2000); Bizzarro et al. (2004); CAIs: MacPherson et al. (1995); Imai & Yurimoto (2000); Itoh et al. (2002); Amelin et al. (2002); Hsu et al. (2003); Kita et al. (2004); Chondrules: Hutcheon & Hutchison (1989); Russell et al. (1996); Kita et al. (2000); McKeegan et al. (2000b); Huss et al. (2001); Yurimoto & Wasson (2003); Kunihiro et al. (2004); Kurahashi et al. (2004); Kita et al. (2005).

Extensive studies on chondrule ^{26}Al chronology were led by the pioneering work of Hutcheon, Huss, & Wasserburg (1994) and Russell et al. (1996). The latter authors observed resolvable ^{26}Mg excesses in two Al-rich chondrules from UOCs, with relative ages of ~ 2 My after CAIs. These authors also reported the lack of excess ^{26}Mg from many other Al-rich chondrules, and inferred an extended period of chondrule formation between 2 to more than 6 My after CAIs. In a subsequent study, Huss et al. (2001) suggested that the apparently younger ages of some chondrules could be the result of parent body metamorphism, rather than representing primary formation ages. Al-rich chondrules and POIs in C chondrites showed similar results with relative ages of 2-3 My or longer after CAIs (Sheng et al. 1991; Hutcheon, Krot, & Ulyanov 2000; Srinivasan, Huss, & Wasserburg 2000; Hsu et al. 2003; Kita et al. 2004). Hutcheon et al. (2000) also suggested that the fraction of Al-rich chondrules without detectable ^{26}Mg excesses increases with increasing degree of metamorphism of the host meteorite. The recent study of Yamato 81020 (CO3.0), showing evidence of ^{26}Al in every chondrule studied, is particularly noteworthy in this regard (Yurimoto & Wasson 2003; Kunihiro et al. 2004; Kurahashi et al., 2004). Therefore, it is very important to work on the least metamorphosed chondrites (types 3.0-3.1) to obtain primary crystallization ages of chondrules.

The first evidence of live ^{26}Al in more common ferromagnesian chondrules was provided by Kita et al. (2000), who measured glassy mesostasis among Ca-pyroxene microcrystalites in type II chondrules from Semarkona. Data for more than 40 ferromagnesian chondrules now indicate that formation of chondrules took place between ~ 1 and ~ 3 My after CAIs (LL3.0-3.1 Semarkona, Bishunpur and Krymka; Hutcheon & Hutchison 1989; Kita et al. 2000; McKeegan et al. 2000b, Mostefaoui et al. 2002; Kita et al. 2005, and CO3.0 Y81020; Yurimoto & Wasson 2003; Kunihiro et al. 2004; Kurahashi et al. 2004). Chondrules from carbonaceous chondrites and ordinary chondrites show significant differences in their oxygen isotopic compositions and their bulk chemical compositions. However, the total range of chondrule formation times (1-3 My) is the same for both chondrite classes. These results strongly indicate chondrules in LL and CO chondrites formed in two regions of the protoplanetary disk that were isolated from each other, but which underwent chondrule formation events at the same time. For LL3 chondrites, Mostefaoui et al. (2002) reported that there is a hint that olivine-rich chondrules are systematically older than pyroxene-rich ones. This is the first indication of a correlation between ages and properties of chondrules. Tachibana et al. (2003) further reported that these chondrule ages correlate with bulk Mg/Si ratios, implying chemical fractionation of chondrule precursors with time in the protoplanetary disk. For CO3.0 chondrite Y81020, a limited number of data imply that type II chondrules are systematically younger than type I in the same meteorite (Yurimoto & Wasson 2003; Kunihiro et al. 2004; Kurahashi et al. 2004). Although chondrules in LL3 and CO3 chondrites seem to show different chemical correlations with the ^{26}Al systematics, the formation ages for the two classes show similar spreads.

The Al-Mg ages discussed above were obtained by SIMS, and the analyses were made of glass and plagioclase, which are the first phases to melt in chondrules. Many chondrules are considered to be recycled (or remelted) from previous generations (Nagahara 1981; Jones 1996) and ^{26}Mg excess accumulated in small Al-rich areas could be easily erased. Therefore, these ^{26}Al ages should be considered to date the last melting events and may not be identical to the time distribution of chondrule forming events (cf Fig. 5). Bizzarro et al. (2004) recently reported high precision ICP-MS ^{26}Al - ^{26}Mg analyses of micro-drilled Allende chondrules. Data for 15 chondrules show model initial $^{26}\text{Al}/^{27}\text{Al}$ ratios ranging from $(1.4 \pm 0.5) \times 10^{-5}$ to values as high as $(5.7 \pm 0.8) \times 10^{-5}$, systematically higher than SIMS and other MC-ICPMS data for chondrules in the same meteorite. At face value, the Bizzarro et al. (2004) results suggest chondrule formation began contemporaneously with CAI formation and continued for at least 1.5 My. Because the bulk Al-Mg system can be preserved during the melting of chondrules, these data likely only indicate the time of formation of chondrule precursors. Alternatively, they may not have any chronological implications if they are produced by simple mixing of old CAIs to chondrule precursors (Galy et al. 2000). If chondrule formation actually started as early as formation of CAIs, many older chondrules formed within the first million years must have been lost or recycled, as suggested by younger SIMS ^{26}Al ages that may correspond to the last chondrule melting events. More study is needed on less-metamorphosed samples to compare the results from bulk and internal analyses.

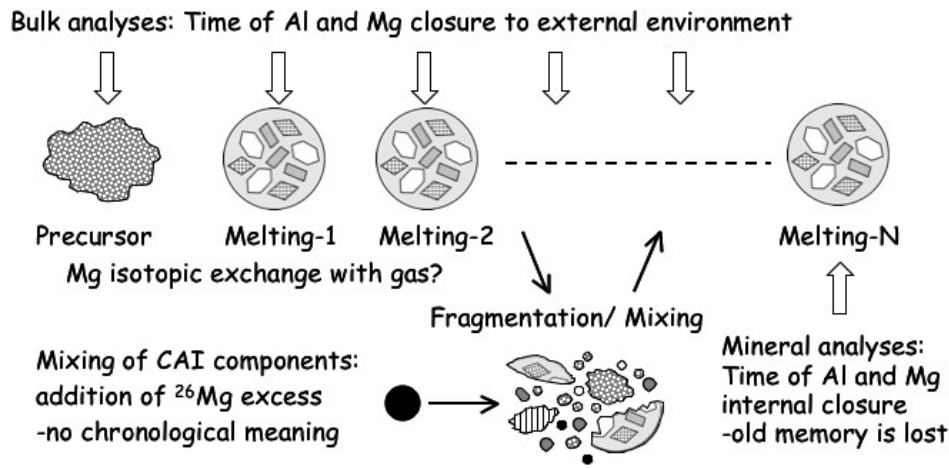


Figure 5. Events dated by different analytical method.

2.3. ^{53}Mn - ^{53}Cr System

The first suggestion of the former presence of ^{53}Mn was derived from ^{53}Cr deficits in low Mn/Cr fractions of CAIs, by interpreting the deficits as due to the early formation of CAIs before ^{53}Cr was added to the solar system from ^{53}Mn decay (Birck & Allègre 1985). The linear trend made by CAIs and bulk host chondrite data on the ^{53}Mn - ^{53}Cr isochron diagram implied an initial $^{53}\text{Mn}/^{55}\text{Mn}$ ratio of 4.4×10^{-5} . However, the $^{53}\text{Mn}/^{55}\text{Mn}$ initial ratio estimated from CAIs is not currently considered to represent the initial solar system value for two reasons. First, the ^{53}Cr deficit is associated with a ^{54}Cr anomaly of nucleosynthetic origin, making it difficult to distinguish between radiogenic and nucleogenetic sources. Nyquist et al. (2003) argued that the source of the ^{53}Cr deficit in CAIs could be very refractory spinels that preserved the early Cr isotopic heterogeneity of the solar system. Second, a Mn-Cr chronology based on the CAI value is inconsistent with high precision Pb-Pb ages for differentiated meteorites (Lugmair & Galer 1992; Nyquist et al. 1994) as well as with the recent Al-Mg ages for chondrules discussed above. Because the initial ^{53}Mn abundance in CAIs is not well understood, ^{53}Mn - ^{53}Cr time scale is now commonly expressed relative to the age of the LEW86010 angrite as follows:

$$\Delta t = \frac{1}{\lambda_{53}} \ln \left\{ \frac{(^{53}\text{Mn}/^{55}\text{Mn})_{\text{LEW86010}}}{(^{53}\text{Mn}/^{55}\text{Mn})_{\text{Sample}}} \right\} \quad (6),$$

where λ_{53} is the decay constant of ^{53}Mn . Applying the high precision Pb-Pb ages of CAIs and LEW86010 (4567.2 ± 0.6 Ma and 4557.8 ± 0.5 Ma, respectively; Amelin et al. 2002; Lugmair & Galer 1992) shows that ^{53}Mn ages calculated from Eq. (6) are offset from ages referenced to CAIs by 9.4 ± 0.8 My.

Nyquist et al. (2001) obtained whole chondrule ^{53}Mn - ^{53}Cr isochrons from Bishunpur and Chainpur (LL3.1) giving initial $^{53}\text{Mn}/^{55}\text{Cr}$ ratios of $(9.4 \pm 3.1) \times 10^{-6}$ and

$(9.5 \pm 1.7) \times 10^{-6}$, respectively (Fig. 6). By applying Eq. (6), these initial ratios correspond to ages 10 Myr older than LEW86010 with errors of 1-2 Myr, which is very similar to the time of CAI formation. An additional Mn-Cr isochron also has been determined for Semarkona chondrules (Fig. 6, JSC unpublished data, also discussed in Nyquist et al. 2003) that gives an initial $^{53}\text{Mn}/^{55}\text{Mn}$ ratio of $(5.8 \pm 1.9) \times 10^{-6}$. This relatively lower value indicates an age 7.5 ± 2.1 Myr older than LEW86010, which is consistent with ^{26}Al ages of chondrules that are ~ 2 Myr after CAIs. Note that these two $^{53}\text{Mn}/^{55}\text{Mn}$ estimates are relatively imprecise and agree within analytical uncertainties. Shukolyukov, Lugmair, & Bogdanovski (2003) obtained an initial $^{53}\text{Mn}/^{55}\text{Mn}$ ratio from bulk carbonaceous chondrites of $(8.5 \pm 1.5) \times 10^{-6}$. This value also coincides with the chondrule data, although the chronological interpretation is questionable because the ^{53}Cr excesses in these samples are correlated to the ^{54}Cr isotopic anomaly from a stellar nucleosynthetic origin.

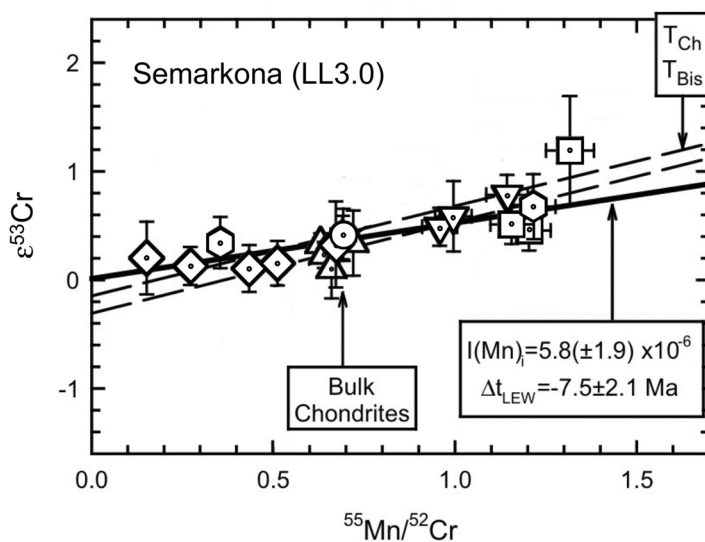


Figure 6. Mn-Cr isochron diagram for chondrules from Semarkona (LL3.0) (Nyquist et al., unpublished). Y axis: $\epsilon^{53}\text{Cr}$ is excess ^{53}Cr in parts in 10^4 compared to the terrestrial value. Triangles: bulk chondrites (Nyquist et al. 2001); diamonds: PO, hexagons: BO, circles: POP, inverted triangles: PP, and squares; RP. T_{CH} and T_{BIS} are isochrones from chondrules in Chainpur (LL3.4) and Bishunpur (LL3.1) (Nyquist et al. 2001).

To aid interpretation of the isotopic data, Nyquist et al. (2001) obtained the major and trace element concentrations in the chondrules that were used for Mn-Cr study, and argued that the concentrations of Na, Fe, and Sc were not fractionated during chondrule formation, hence, that the initial $^{53}\text{Mn}/^{55}\text{Mn}$ ratios represented those in the precursors. They also found that the relative abundances of Sc, Mn, and Cr form a well-defined trend (Fig. 7), consistent with volatility-controlled elemental abundances where volatility increases in the order $\text{Sc} < \text{Cr} < \text{Mn}$ (see Fig. 2a). The most

volatile element, Mn, is depleted in Type IA porphyritic olivine (PO) chondrules, but is preferentially enriched in radial pyroxene (RP) chondrules. The trend further extends to the composition of refractory forsterites (RFs) from Allende, having compositional characteristics determined by condensation from the solar nebula (Weinbruch, Palme, & Spettel 2000). RFs might form in a well-defined, very-reducing, high-temperature environment, provided either by direct condensation from the solar nebula, or by crystallization from very refractory melts, only slightly less refractory than the parental melts of CAIs (Palme et al. 2004). It is from these elemental trends that Nyquist et al. (2001) suggested that the bulk Mn-Cr isochrons of chondrules characterize the time when chondrule precursors were forming in the solar nebula. The nearly equivalent value of $^{53}\text{Mn}/^{55}\text{Mn} = (8.5 \pm 1.5) \times 10^{-6}$ obtained for bulk carbonaceous chondrites (Shukolyukov et al. 2003) is consistent with the very plausible assumption that carbonaceous chondrites are derived from early, primitive materials in the solar nebula accreted on undifferentiated asteroids.

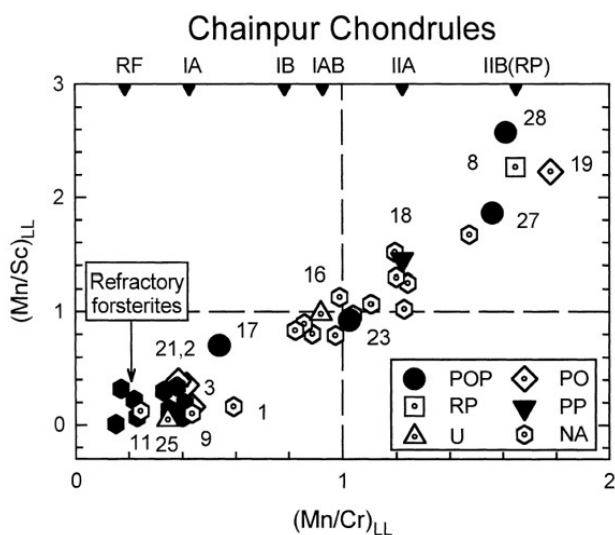


Figure 7. LL-chondrite-normalized Mn/Cr and Mn/Sc ratios for Chainpur chondrules studied by Nyquist et al. (2001). The abundance of Mn, Cr and Sc was obtained by instrumental neutron activation analyses. Data for refractory forsterites (RF) are from Weinbruch et al. (2000). More refractory compositions are at the lower left in the figure, less refractory compositions are at the upper right.

2.4. ^{60}Fe - ^{60}Ni System

Iron-60 decays to ^{60}Ni with a half-life of ~ 1.5 My, the shortest among the short-lived nuclides that are only made in stars; ^{60}Fe , ^{92}Nb , ^{129}I , ^{146}Sm , ^{182}Hf , and ^{244}Pu . Thus, ^{60}Fe is a key to understanding the origin of the short-lived nuclides in the solar system (see Goswami et al. this volume). Detecting evidence for ^{60}Fe in solar system materials is quite challenging. The daughter isotope, ^{60}Ni , is the second most abun-

dant nickel isotope at 26.22%, so the isotopic effects of ^{60}Fe decay must be identified as small additions to a large isotopic bucket. This requires either very-high-precision data or very favorable Fe/Ni ratios.

The first hint for ^{60}Fe in solar system materials was found in Allende CAIs (Birck & Lugmair 1988). Small excesses of ^{60}Ni found in several inclusions were tentatively attributed to the decay of ^{60}Fe , corresponding to an initial $^{60}\text{Fe}/^{56}\text{Fe}$ ratio of 1.6×10^{-6} at the time that CAIs crystallized (Birck & Lugmair 1988). However, these excesses were in some cases accompanied by excesses in ^{64}Ni and ^{62}Ni , which are best explained as residual nucleosynthetic anomalies from a stellar source, as in the case of the ^{54}Cr anomaly in CAIs. The first evidence that ^{60}Fe was alive in the early solar system was found in the Chervony Kut and Juvinus eucrites, basaltic meteorites consisting of minerals with very high Fe/Ni ratios (up to $\sim 3 \times 10^3$) due to preferential partitioning of Ni into the parent asteroid's metallic core (Shukolyukov & Lugmair 1993a, b, 1996). The $^{60}\text{Fe}/^{56}\text{Fe}$ ratios inferred for the eucrites are significantly lower than that inferred for Allende CAIs and also differ significantly from one another (Chervony Kut = $(3.9 \pm 0.6) \times 10^{-9}$; Juvinas = $(4.3 \pm 1.5) \times 10^{-10}$). The large difference in initial $^{60}\text{Fe}/^{56}\text{Fe}$ for the eucrites contrasts with their similar initial $^{53}\text{Mn}/^{55}\text{Mn}$ ratios (Lugmair & Shukolyukov 1998), implying that the ^{60}Fe - ^{60}Ni system is more susceptible to secondary disturbance than is the ^{53}Mn - ^{53}Cr system (Lugmair & Shukolyukov 1998).

More-recent attempts to find evidence of ^{60}Fe in CAIs and chondrules by the ion microprobe technique were not successful in detecting resolvable ^{60}Ni excess (Choi, Huss, & Wasserburg 1999; Kita et al. 2000). The first clear evidence for ^{60}Fe in chondrites came from SIMS measurements on troilite (FeS) in Bishunpur, Krymka (LL3.1), and Semarkona (Tachibana & Huss 2003; Mostefaoui et al. 2004, 2005). The high Fe/Ni ratios for the troilites (up to 2×10^5 for Bishunpur and Krymka and up to 5×10^4 for Semarkona) made it possible to detect ^{60}Ni excesses. The inferred $^{60}\text{Fe}/^{56}\text{Fe}$ ratios for Bishunpur and Krymka troilites were in the range of $1\text{--}2 \times 10^{-7}$, from which Tachibana & Huss (2003) inferred a $(^{60}\text{Fe}/^{56}\text{Fe})$ ratio for the early solar system of $(2.8\text{--}4) \times 10^{-7}$. An isochron for Semarkona troilites gave a significantly higher $^{60}\text{Fe}/^{56}\text{Fe}$ ratio of $(0.92 \pm 0.24) \times 10^{-6}$ (Mostefaoui et al. 2005). These authors consider this value to be the minimum estimate for the initial ratio of the solar system. Once it was clear that ^{60}Fe had been present in chondrites and could be detected in sulfides, Guan et al. (2003a) and Guan, Huss, & Leshin (2003b) measured sulfides in type 3 enstatite chondrites for both ^{60}Fe - ^{60}Ni and ^{53}Mn - ^{53}Cr systematics. They found clear evidence of ^{60}Fe and ^{53}Mn in many of the sulfides. However, the initial $(^{60}\text{Fe}/^{56}\text{Fe})$ ratios ranged from $\sim 1 \times 10^{-7}$ to $\sim 1 \times 10^{-5}$, even among sulfides from the same meteorite! Mn-Cr "isochrons" were also quite variable from grain to grain and did not closely correlate with the $(^{60}\text{Fe}/^{56}\text{Fe})$ ratios. It seems clear that many, if not all, of the sulfides in enstatite chondrites experienced parent body temperatures of $\sim 500^\circ\text{C}$ (similar to temperature experienced by Qingzhen, EH3; Huss & Lewis 1994) and do not preserve the $^{60}\text{Fe}/^{56}\text{Fe}$ ratio in the solar nebula when the sulfides originally formed (Guan et al. 2003a, b; Guan, Huss, & Leshin 2004).

Faced with unreliable sulfide data from enstatite chondrites, one must consider the possibility that the ^{60}Fe - ^{60}Ni system for sulfides in other meteorites may have also been reset or disturbed, even those from the least metamorphosed ordinary chondrites. It is therefore important to find evidence for ^{60}Fe in minerals that are less sus-

ceptible to thermal resetting. Two non-sulfide minerals in chondrites have now shown evidence for ^{60}Fe . In Semarkona, magnetite (Fe/Ni up to 6×10^5), a secondary mineral most likely produced by aqueous alteration on the parent body, gives $^{60}\text{Fe}/^{56}\text{Fe} \approx 1.4 \times 10^{-7}$ (Mostefaoui et al. 2004, 2005). FeO-rich pyroxene chondrules from Semarkona and Bishunpur (Fe/Ni up to 3×10^4) give $^{60}\text{Fe}/^{56}\text{Fe} \approx (2-4) \times 10^{-7}$ (Fig. 8) (Huss & Tachibana 2004; Tachibana et al. 2005). Although there have been no data on Fe-Ni diffusion in orthopyroxene, if we assume that the Fe-Ni diffusion rate in orthopyroxene is similar to that for Fe-Mg (Ganguly & Tazzoli 1994), the closure temperature for several micron-sized pyroxene would be higher than 1000°C when the chondrule melt was cooled at the rate of 100 K/hr. Semarkona and Bishunpur have experienced metamorphic temperatures no higher than $\sim 260^\circ\text{C}$ and $\sim 300^\circ\text{C}$, respectively (e.g., Rambaldi & Wasson 1981; Alexander et al. 1989; Huss & Lewis 1994), most likely much too low for significant diffusion of Fe and Ni. The metamorphic temperatures experienced by Semarkona do not seem to have affected the chondrule silicates (e.g., Grossman & Brearley 2005). Thus, in Semarkona and Bishunpur, silicates are likely to preserve evidence of the original $^{60}\text{Fe}/^{56}\text{Fe}$ ratios acquired during chondrule formation, while magnetite in Semarkona may record the timing of parent body aqueous alteration. So far, non-sulfides have not given the high $^{60}\text{Fe}/^{56}\text{Fe}$ ratios observed in Semarkona troilites.

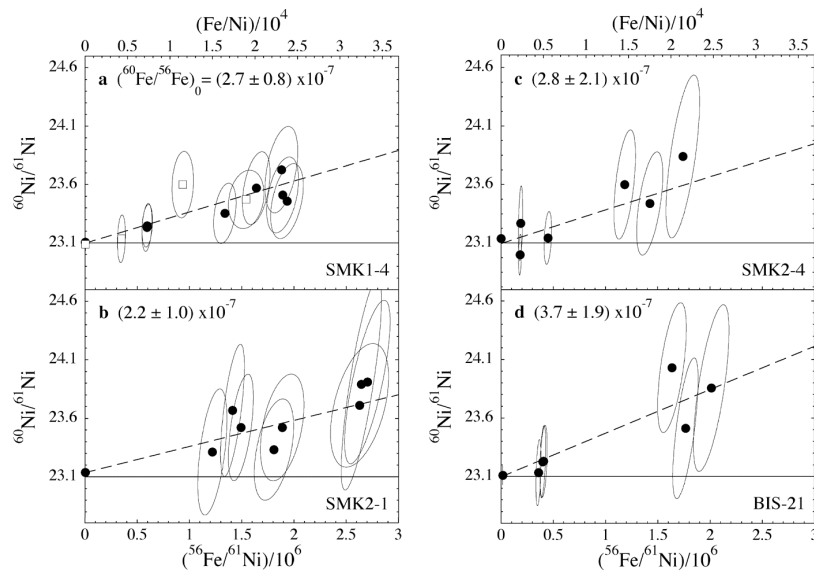


Figure 8. The ^{60}Fe - ^{60}Ni isochron of FeO-rich pyroxene chondrules in Semarkona (SMK1-4, 2-1, 2-4) and Bishunpur (BIS-21), after Tachibana et al. (2005).

Although the current data are very limited, some first order chronological interpretations are possible. Two different interpretations can be constructed for Semarkona depending on which data one thinks are most reliable. One starting point is to assume that the high $^{60}\text{Fe}/^{56}\text{Fe}$ ratio inferred for Semarkona troilites, $(0.92 \pm 0.24) \times 10^{-6}$ by Mostefaoui et al. (2005) is the best value for formation of the main constituents of

chondrites. Mostefaoui et al. (2005) concluded that troilite data from Semarkona (LL3.0) are free from secondary effects because they measured metal-free troilite where diffusive exchange of isotopes and elements are extremely limited. An initial $^{60}\text{Fe}/^{56}\text{Fe}$ ratio for the solar system can be inferred by assuming that the troilites are contemporaneous with the chondrules in Semarkona and formed ~ 1 My after CAIs (e.g., Kita et al. 2000). The calculated initial $^{60}\text{Fe}/^{56}\text{Fe}$ ratio for the solar system is then very similar to the $^{60}\text{Fe}/^{56}\text{Fe}$ ratio inferred for CAIs (1.6×10^{-6} ; Birck & Lugmair 1988). The Semarkona chondrule with evidence of ^{60}Fe is then constrained to have formed, or to have been last altered ~ 4 My after the Semarkona troilite. In this interpretation, the Semarkona chondrule cannot be recording the formation of the majority of chondrules in the meteorite. The Semarkona magnetite is constrained to have formed ~ 0.75 My after the Semarkona chondrule, or ~ 4.75 My after CAIs. This time line implies that an extended period of accretion and parent body alteration is recorded in Semarkona.

An alternative timeline assumes that FeO-rich pyroxene chondrules contain the most reliable record of the $^{60}\text{Fe}/^{56}\text{Fe}$ ratio at the time the majority of chondrules formed. If so, then the inferred initial $^{60}\text{Fe}/^{56}\text{Fe}$ ratio for the earliest epoch of the solar system, when CAIs formed, was 5×10^{-7} - 1×10^{-6} (Huss & Tachibana 2004; Tachibana et al. 2005). Many sulfides and most magnetites in Semarkona are secondary, having formed during parent body aqueous alteration (e.g., Krot et al. 1997). The secondary sulfides are typically Ni-rich (i.e., Fe-poor). In this interpretation, the $^{60}\text{Fe}/^{56}\text{Fe}$ ratios inferred for the pyroxene-rich chondrules record the time of chondrule formation, and the Fe-Ni data for Semarkona magnetite reflects the time of parent-body aqueous alteration. The time interval between chondrule formation and magnetite formation, during which accretion of the parent body would have taken place, was 0.75 My. The Semarkona sulfides have lost iron and do not give a reliable record of $^{60}\text{Fe}/^{56}\text{Fe}$ at the time when the major constituents of Semarkona formed, and the $^{60}\text{Fe}/^{56}\text{Fe}$ ratio inferred from uncorrelated ^{60}Ni excesses in CAIs are not due to *in situ* decay of ^{60}Fe . The sulfides in Bishunpur and Krymka may not have experienced sufficient aqueous alteration to cause iron loss, but instead may have recorded gentle thermal metamorphism in the host meteorites that reset their isotopic clocks 0.5-1 My after chondrules formed.

The database for ^{60}Fe is likely to grow rapidly over the next few years. Target minerals have been identified, and the new generation of high-transmission ion microprobes makes possible the measurements of the small excesses of ^{60}Ni in phases with relatively low Fe/Ni ratios (e.g., chondrule olivine). The ^{60}Fe - ^{60}Ni system could well provide the bridge that permits cross correlation of the ^{26}Al - ^{26}Mg and ^{53}Mn - ^{53}Cr systems to give a coherent chronological picture of the early solar system, and may also provide some insights into the stellar contribution to the short-lived nuclides in the early solar system.

3. Implications for the History of the Protoplanetary Disk

3.1. Comparison of Multiple Chronometers and an Overview of Meteorite Ages

Initial homogeneity in the abundances of short-lived nuclides throughout the early solar nebula is necessarily assumed in order to apply the short-lived radionuclide

chronometers. One way to test the validity of this assumption is to compare the ages of individual meteorites as dated by various short-lived chronometers and the Pb-Pb method. Figure 9 compares three chronometers, Pb-Pb, Al-Mg, and Mn-Cr, for various types of meteorite samples. In many cases, these chronometers agree well within analytical uncertainties, suggesting that ^{26}Al and ^{53}Mn were reasonably homogeneous in the early solar nebula, at least in the asteroid belt. The possible ^{53}Mn heterogeneity in the solar system as a function of heliocentric distance (Lugmair & Shukolyukov 1998) would appear to be only a second-order effect. There are some minor inconsistencies in Figure 9, which could be interpreted as initial isotopic heterogeneity of these nuclides (e.g., Gounelle & Russell 2005). However, these could be due to differences in closure temperatures for different chronometers, especially if the parent bodies were slowly cooled and/or experienced some form of thermal processing (due to meteorite impacts, etc.) at later times. It should be noted that igneous clasts in polymict ureilites (impact breccias containing fragments of both host ureilites and exotic materials) show consistent ^{26}Al and ^{53}Mn ages in Figure 9 within analytical errors of 0.4 My (Goodrich, Hutcheon, & Keil 2002; Kita et al. 2003). Both chronometers might reflect closed-system behavior since their crystallization because these meteorites preserve well their fast-cooled igneous textures (Ikeda, Prinz, & Nehru 2000).

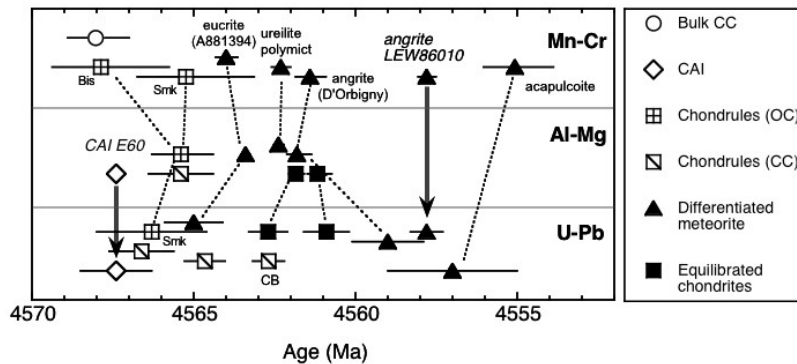


Figure 9. Comparison of three chronometers. The relative Al-Mg and Mn-Cr ages are converted to absolute ages using Pb-Pb ages obtained for CAI E60 (4567.2 ± 0.6 Ma; Amelin et al. 2002) and LEW86010 angrite (4557.8 ± 0.5 Ma; Lugmair & Galer 1989), respectively. Dashed lines connect the data obtained from the same meteorites. “Smk” and “Bis” indicate chondrules from Semarkona and Bishunpur meteorites, respectively. Chondrule Al-Mg data represent the range shown in Figure 4. Other data are from Shukolyukov et al. (2003), Nyquist et al. (2001, 2003, unpublished), Jagoutz et al. (2003), Wadhwa et al. (2005), Goodrich et al. (2002), Kita et al. (2003), Göpel et al. (1992), Lugmair & Shukolyukov (1998), Göpel, Manhès, & Allègre (1994), Zinner & Göpel (2002), Amelin et al. (2004; unpublished), Krot et al. (2005).

Overall, the data for the meteorites show that there is a preferred order of ages, from CAIs, to chondrules, and then to planetary-differentiated meteorites and thermally equilibrated chondrites. The time period of this evolution is comparable to the time period of protostar, classical T Tauri, and weak-lined T Tauri stages of low mass

stars (Calvet et al. 2000). A short time scale of no more than a half My is inferred for the formation of a variety of CAIs with similar initial $^{26}\text{Al}/^{27}\text{Al}$ ratios near the canonical value of 5×10^{-5} , implying that they formed during the protostar stage when the protoplanetary disk was very active due to high accretion rates. Chondrules formation began within 1.5 My after CAIs, which are similar to the average lifetime of the classical T Tauri stage for low mass stars and may represent the lifetime of the protoplanetary disk. Furthermore, ^{26}Al ages among chondrules in the same chondrites vary by least 1 My (see Fig. 4), indicating chondrule-forming events must have been repeated many times over an interval of about a million years. The earliest differentiated meteorites postdated the youngest chondrule ages by only ~ 1 My or less, and in some cases they overlap within analytical uncertainties. These results may also indicate that chondrules present in most chondrites formed in the protoplanetary disk and predated the planetary accretion, rather than on a parent body as suggested by Hutchison, Williams, & Russell 2001; Hutchison, Bridges, & Gilmour, this volume). Certain types of chondrules, for example those present in CB chondrites (Krot et al. 2005a), probably formed by processes involving large planetesimals (e.g., Weidenschilling, Marzari, & Hood 1998). Through rapid growth of planetesimals (≤ 1 My; e.g., Kortekamp, Kokubo, & Weidenschilling 2000) and melting and differentiation due to heat generated by the decay of ^{26}Al and ^{60}Fe , basalt formation started quickly in early-formed asteroidal bodies.

The above picture drawn from meteorite ages implies that the onset of planetary formation was delayed by one My or more after formation of the first solids. Many dynamic models indicate a short time-scale of less than a million years for protoplanet formation after the turbulence in the protoplanetary disk became weak enough to permit formation of a gravitationally unstable thin disk (see Cuzzi et al., this volume). This apparent discrepancy between dynamic models and the meteorite record points to the need for collaborations between the two communities.

3.2. Chondrules from Ordinary Chondrites: Did Volatile Element Abundance Increase with Nebular Residence Time?

As described earlier, the initial $^{26}\text{Al}/^{27}\text{Al}$ ratios of chondrules from LL3.0-3.1 chondrites (the least equilibrated ordinary chondrites) seem to correlate with bulk Si/Mg ratios (Fig. 10). Tachibana et al. (2003) and Tomomura et al. (2004) showed that bulk Si/Mg ratios correlate with the abundance of moderately volatile elements, such as Mn and Na. Tachibana et al. (2003) suggested a mechanism for enhancing the volatile content of later-formed chondrules by repeated chondrule formation accompanying gas/solid fractionation for Mg, Si, and other volatile elements (Fig. 11). They suggested that Si was selectively lost from earlier generations of chondrules because Si is more volatile than Mg and evaporates more rapidly from a chondrule melt. Open system behavior of Si during chondrule formation is also suggested from SiO_2 enrichment at the periphery of chondrules (Krot et al. 2003; Libourel, Krot, & Tissandier 2005). If these early-formed Mg-rich chondrules were separated from the chondrule-forming region and the evaporated Si-rich materials was added to the next generation of chondrule precursors as fine grained recondensed dust, the chondrule precursors would become more Si rich than earlier precursors. By repeating this process many times, the later-formed chondrules would become progressively more

Si- and volatile-rich than early formed ones. Nakamoto et al. (2005; also in this volume) presented a new model for chondrule-forming shockwave that can be generated by X-ray flare of the young sun. In this model, chondrule precursors should be lifted to upper region of the solar nebula (\sim one scale height) by turbulence and heated by the shockwave. Volatile elements would have evaporated during melting, recondensed into fine-grained dust, and then would have been enriched in upper region of the disk, while newly formed chondrules might be returned to midplane of the disk. This new model has a potential to explain the observed age-composition relationship among chondrules in LL3.

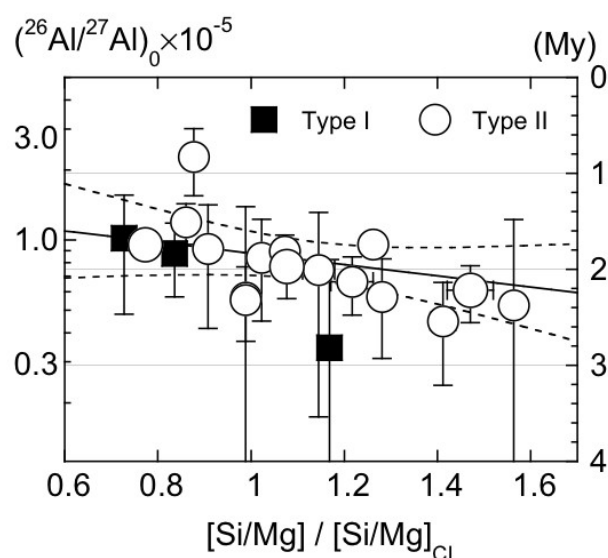


Figure 10. Correlation of ^{26}Al ages with bulk Si/Mg ratios for chondrules from LL3.0-3.1 chondrites. After Tachibana et al. (2003) and Kita et al. (2005).

Because Mn and Cr are more volatile than Si (Fig. 2a), the process of Si-enrichment proposed by Tachibana et al. (2003) might also have changed the bulk Mn and Cr abundance of the chondrules. As described in the previous section, Nyquist et al. (2001) observed Mn/Cr enrichments in pyroxene rich chondrules from LL3 chondrites. If chondrules formed over a period of time from a gas that is continually enriched Mn relative to Cr by chondrule formation, later-formed chondrules would be more Mn rich and would acquire lower $^{53}\text{Mn}/^{55}\text{Mn}$ ratios. In this scenario, the bulk ^{53}Mn - ^{53}Cr data of chondrules would not plot exactly on a single isochron, but approximately on the isochron, and would show a time delay relative to CAI formation similar to that shown by the ^{26}Al ages of the chondrules (\sim 2 My after CAIs). Currently available bulk Mn-Cr data do not resolve the \sim 2 My time difference, indicating ages both similar to CAIs (Chainpur and Bishunpur, Nyquist et al. 2001) and

~2 My after CAIs (Semarkona, Nyquist et al. unpublished). More work should be done to answer the question.

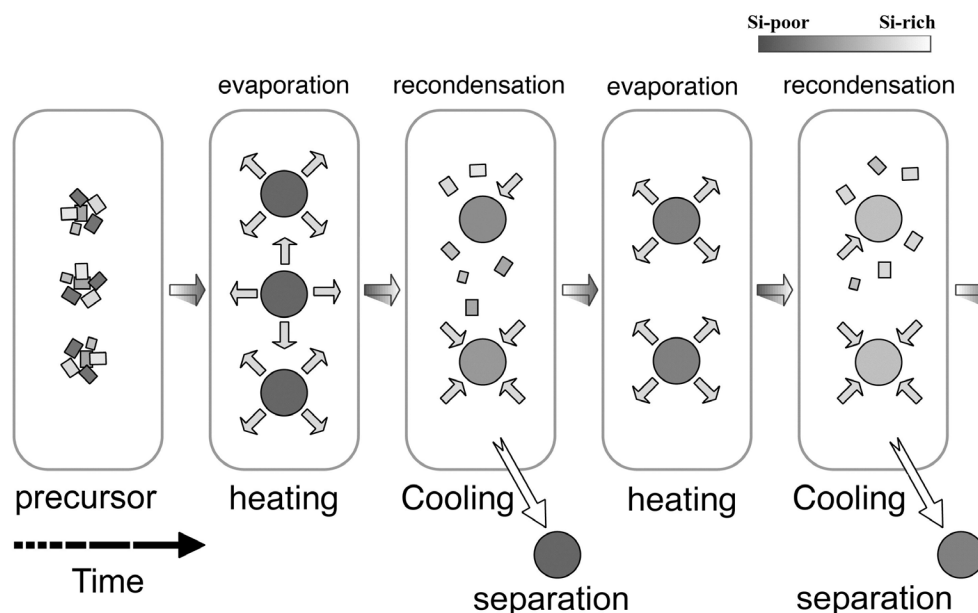


Figure 11. Volatile enrichment in later formed chondrules (Tachibana et al. 2003).

4. Concluding Remarks

Over the last 5-10 years, many of new data from high precision chronometers were obtained that focused on the earliest epoch of solar system history. The analyses of specific meteorites by multiple chronometers provided broadly consistent results, validating the general usefulness of the short-lived chronometers. At the same time, the chronometers based on short-lived nuclides often do not agree in detail for reasons that remain poorly understood. A major focus of future research in meteorite chronology is to understand the apparent discrepancies between chronometers and, using this information, to develop new constraints on early solar system history.

Future studies on meteorite chronology should address the time difference between CAI formation and chondrule formation and the spread in formation times among CAIs and chondrules. The mechanisms of CAI and chondrule formation are still being debated, and there is a lack of consensus as to whether CAI and chondrule formation periods overlapped. Oxygen isotopes in bulk chondrules are not as ^{16}O -rich as CAIs, indicating the environments of their formation were not the same (see McKeegan et al. 2004; Russell et al.; MacPherson et al., and Jones et al. this volume). If the age data clearly demonstrate separate formation periods, such as CAI formation within a few times 10^5 yr of "time zero", while chondrules began forming ~1 My later, either the formation mechanisms were different, or there were large differences

in the environments of the two events. The chronology of CAIs is still perplexing in detail as we have to examine a small time difference on the order of 0.1 My. Concerns over isotopic heterogeneity and/or disturbance of both parent and daughter nuclides also require much greater attention. Many short-lived nuclides might have been injected by a supernova into the molecular cloud from which the solar system formed (Goswami et al. this volume) or could have been injected to the existing disk (Ouellette, Desch, & Hester, this volume). In addition to ^{10}Be , some portion of the other nuclides could also have been produced by irradiation in the solar system (Goswami et al., this volume). The process of isotopic homogenization of short-lived nuclides in the solar nebula is also an area that needs more investigation.

Acknowledgments. We appreciate constructive reviews by Mini Wadhwa, Andy Davis, Glenn MacPherson (AE), and Sasha Krot (Editor), which significantly improved the contents and clarity of the paper.

References

- Alexander, C. M. O'D., Barber, D. J., & Hutchison, R. H. 1989, *Geochim. Cosmochim. Acta*, 53, 3045
- Allègre, C. J., Manhès, G., & Göpel, C. 1995, *Geochim. Cosmochim. Acta*, 59, 1445
- Amelin, Y. 2005, *Meteorit. Planet. Sci.*, in press
- Amelin, Y., Krot, A. N., Hutcheon, I. D., & Ulyanov, A. A. 2002, *Science*, 297, 1678
- Amelin, Y., Krot, A., & Twelker, E. 2004, *Geochim. Cosmochim. Acta*, 68, A759
- Amelin, Y., Ghosh, A., & Rotenberg, E. 2005, *Geochim. Cosmochim. Acta*, 69, 505
- Begemann, F., Ludwig, K. R., Lugmair, G. W., Min, K., Nyquist, L. E., Patchett, P. J., Renne, P. R., Shih, C.-Y., Villa, I. M., & Walker, R. J. 2001, *Geochim. Cosmochim. Acta*, 65, 111
- Birck, J. L., & Allègre, C. J. 1985, *Geophys. Res. Lett.*, 12, 745
- Birck, J. L., & Lugmair, G. W. 1988, *Earth Planet. Sci. Lett.*, 90, 131
- Bischoff, A., & Keil K. 1984, *Geochim. Cosmochim. Acta*, 48, 693
- Bizzarro, M., Baker, J. A., & Haack, H. 2004, *Nature*, 431, 275
- Caillet, C., MacPherson, G. J., & Zinner, E. K. 1993, *Geochim. Cosmochim. Acta*, 57, 4725
- Calvet, N., Hartmann, L., & Strom, S. E. 2000, in *Protostars and Planets IV*, eds. V. Mannings, A. P. Boss, & S. S. Russell (Tucson: Univ. Arizona Press), 377
- Chen, J. H., & Tilton, G. R. 1976, *Geochim. Cosmochim. Acta*, 40, 635
- Chen, J. H., & Wasserburg, G. J. 1981, *Earth Planet. Sci. Lett.*, 52, 1
- Choi, B.-G., Huss, G. R., & Wasserburg, G. J. 1999, *Lunar Planet. Sci.*, 30, 2004
- Davis, A. M., Richter, F. M., Mendybaev, R. A., Janney, P. E., Wadhwa, M., & McKeegan, K. D. 2005, *Lunar Planet. Sci.*, 36, 2334.
- Dickin, A. P. 1995, *Radiogenic Isotope Geology* (Cambridge: Cambridge Univ. Press)
- Ebel, D. S., & Grossman, L. 2000, *Geochim. Cosmochim. Acta*, 64, 339
- Faure, G. 1986, *Principles of Isotope Geology* (New Jersey: John Wiley & Sons)
- Galy, A., Young, E. D., Ash, R. D., & O'Nions, R. K. 2000, *Science*, 290, 1751
- Galy, A., Hutcheon, I. D., & Grossman, L. 2004, *Lunar Planet. Sci.*, 35, 1790
- Ganguly, J., & Tazzoli, V. 1994, *Amer. Mineral.*, 79, 930
- Goodrich, C. A., Hutcheon, I. D., & Keil, K. 2002, *Meteorit. Planet. Sci.*, 37, A54
- Göpel, C., Manhès, G., & Allègre, C. J. 1992, *Meteoritics*, 27, 226
- Göpel, C., Manhès, G., & Allègre, C. J. 1994, *Earth Planet. Sci. Lett.*, 121, 153
- Gray, C. M., & Compston, W. 1974, *Nature*, 251, 495
- Gray, C. M., Papanastassiou, D. A., & Wasserburg, G. J. 1973, *Icarus*, 20, 213

- Grossman, L., & Larimer, J. W. 1974, *Rev. Geophys. Space Phys.*, 12, 71
- Grossman, J. N., & Brearley, A. J. 2005, *Meteorit. Planet. Sci.*, 40, 87
- Gounelle, M., & Russell, S. S. 2005, *Geochim. Cosmochim. Acta*, in press
- Guan, Y., Huss, G. R., MacPherson, G. J., & Wasserburg, G. J. 2000, *Science*, 289, 1330
- Guan, Y., Huss, G. R., Leshin, L. A., & MacPherson, G. J. 2003a, *Meteorit. Planet. Sci.*, 38, A138
- Guan, Y., Huss, G. R., & Leshin, L. A. 2003b, Presented at the NIPR International Symposium, "Evolution of solar system materials: A new perspective from Antarctic Meteorites", 33
- Guan, Y., Huss, G. R., & Leshin, L. A. 2004, *Lunar Planet. Sci.*, 35, 2003
- Hsu, W., Wasserburg, G. J., & Huss, G. R. 2000, *Earth Planet. Sci. Lett.*, 182, 15
- Hsu, W., Wasserburg, G. J., & Huss, G. R. 2003, *Meteoritics Planet. Sci.*, 38, 35
- Huss, G. R., & Lewis, R. S. 1994, *Meteoritics*, 29, 811
- Huss, G. R., & Tachibana, S. 2004, *Lunar Planet. Sci.*, 35, 1811
- Huss, G. R., MacPherson, G. J., Wasserburg, G. J., Russell, S. S., & Srinivasan, G. 2001, *Meteorit. Planet. Sci.*, 36, 975
- Hutcheon, I. D. 1982a, *Amer. Chem. Soc. Symp. Ser.*, 176, 95
- Hutcheon, I. D. 1982b, *Meteoritics*, 17, 230
- Hutcheon, I. D., & Hutchison, R. 1989, *Nature*, 337, 238
- Hutcheon, I. D., Huss, G. R., & Wasserburg, G. J. 1994, *Lunar Planet. Sci.*, 25, 587
- Hutcheon, I. D., Krot, A. N., & Ulyanov, A. A. 2000, *Lunar Planet. Sci.*, 31, 1869
- Hutchison, R., Williams, I. P., & Russell, S. S. 2001, *Phil Trans R. Soc. London A*, 359, 2077
- Ikeda, Y., Prinz, M., & Nehru, C. E. 2000, *Antarct. Meteorite Res.* 13, 177
- Imai, H., & Yurimoto, H. 2000, *Lunar Planet. Sci.*, 31, 1510
- Ireland, T. R., Fahey, A. J., & Zinner, E. K. 1988, *Geochim. Cosmochim. Acta*, 52, 2841
- Itoh, S., Rubin, A. E., Kojima, H., Wasson, J. T., & Yurimoto, H. 2002, *Lunar Planet. Sci.*, 33, 1490
- Jagoutz, E., Jotter, R., Kubny, A., Varela, M. E., Kurat, G., Zartman, R., & Lugmair, G. W. 2003, *Meteorit. Planet. Sci. Suppl.*, 38 Suppl., A81
- Jeffery, P. M., & Reynolds, J. H. 1961 *J. Geophys. Res.*, 66, 3582
- Jones, R. H. 1996, in *Chondrules and the Protoplanetary Disk*, eds. R. H. Hewins, R. H. Jones, & E. R. D. Scott (Cambridge: Cambridge University Press), 163
- Kennedy, A. K., Lofgren, G. E., & Wasserburg, G. J. 1993, *Earth Planet. Sci. Lett.*, 115, 177
- Kita, N. T., Nagahara, H., Togashi, S., & Morishita, Y. 2000, *Geochim. Cosmochim. Acta*, 64, 3913
- Kita, N. T., Ikeda, Y., Shimoda, H., Morishita, Y., & Togashi, S. 2003, *Lunar Planet. Sci.*, 34, 1557
- Kita, N. T., Lin, Y., Kimura, M., & Morishita, Y. 2004, *Lunar Planet. Sci.*, 35, 1471
- Kita, N. T., Tomomura, S., Tachibana, S., Nagahara, H., Mostefaoui, S., & Morishita, Y. 2005, *Lunar Planet. Sci.*, 36, 1750
- Kortekamp, S. J., Kokubo, E., & Weidenschilling, S. J. 2000, in *Origin of the Earth and Moon*, eds. R. M. Canup, & K. Righter (Tucson: Univ. Arizona Press), 85
- Krot, A. N., & Keil K. 2002, *Meteorit. Planet. Sci.*, 37, 91
- Krot, A. N., Zolensky, M. E., Wasson, J. T., Scott, E. R. D., Keil, K., & Ohsumi, K. 1997, *Geochim. Cosmochim. Acta*, 61, 219
- Krot, A. N., Hutcheon I. D., & Keil K. 2002, *Meteorit. Planet. Sci.* 37, 155
- Krot, A. N., Libourel, G., Goodrich, C. A., Petaev, M. I., & Killgore, M. 2003, *Lunar Planet. Sci.*, 34 1451
- Krot, A. N., Amelin, Y., Cassen, P., & Meibom, A. 2005a, *Nature*, in press.
- Krot, A. N., Yurimoto, H., Hutcheon, I. D., & MacPherson, G. J., 2005b, *Nature*, 434, 998
- Kunihiro, T., Rubin, A. E., McKeegan, K. D., & Wasson, J. T. 2004, *Geochim. Cosmochim.*

- Acta, 68, 2947
- Kurahashi, E., Kita, N. T., Nagahara, H., & Morishita, Y. 2004, *Lunar Planet. Sci.*, 35, 1476
- LaTourrette, T., & Wasserburg, G. J. 1998, *Earth Planet. Sci. Lett.*, 158, 91
- LaTourrette, T., & Hutcheon, I. D. 1999, *Lunar Planet. Sci.*, 30, 2003
- Lee, T., & Papanastassiou, D. A. 1974, *Geophys. Res. Lett.*, 1, 225
- Lee, T., Papanastassiou, D. A., & Wasserburg, G. J. 1976, *Geophys. Res. Lett.* 3, 41
- Libourel, G., Krot, A. N., & Tissandier, L. 2005, *Lunar Planet. Sci.*, 36, 1877
- Lin, Y., Guan, Y., Leshin, L. A., Ouyang, Z., & Wang, D. 2004, *Lunar Planet. Sci.*, 35, 2084
- Lodders, K. (2003) *ApJ*, 591, 1220
- Lugmiar, G. W., & Galer, S. J. G. 1992, *Geochim. Cosmochim. Acta*, 56, 1673
- Lugmair, G. W., & Shukolyukov, A. 1998, *Geochim. Cosmochim. Acta*, 62, 2863
- MacPherson, G. J., & Davis, A. M. 1993, *Geochim. Cosmochim. Acta*, 57, 231
- MacPherson, G. J., & Huss, G. R. 2003, *Lunar Planet. Sci.*, 34, 1825
- MacPherson, G. J., Davis, A. M., & Zinner, E. K. 1995, *Meteoritics*, 30, 365
- MacPherson, G. J., Huss, G. R., & Davis, A. M. 2003, *Geochim. Cosmochim. Acta*, 67, 3165
- Marhus, K. K., Goswami, J., Davis, A. M. 2002, *Science*, 298, 2182
- McKeegan, K. D., & Davis, A. M. 2003, in *Meteorites, Comets, and Planets*, ed. Davis, A. M., Vol. 1 *Treatise on Geochemistry*, eds. H. D. Holland, & K. K. Turekian (Oxford: Elsevier), 431
- McKeegan, K. D., Chaussidon, M., & Robert, F. 2000a, *Science*, 289, 1334
- McKeegan, K. D., Greenwood, J. P., Leshin, L. A., & Cosarinsky, M. 2000b, *Lunar Planet. Sci.*, 31, 2009
- McKeegan, K. D., Clayton, R. N., Leshin, L. A., Young, E. D., & Yurimoto, H. 2004, <http://www.lpi.usra.edu/meetings/chondrites2004/pdf/9060.pdf>
- Minster, J. F., Birck, J. L., & Allègre, C. J. 1982, *Nature*, 300, 414
- Mostefaoui, S., Kita, N. T., Tachibana, S., Togashi, S., Nagahara, H., & Morishita, Y. 2002, *Meteorit. Planet. Sci.*, 37, 421
- Mostefaoui, S., Lugmair, G. W., Hoppe, P., & El Goresy, A. 2003, *Lunar Planet. Sci.*, 34, 1585
- Mostefaoui, S., Lugmair, G. W., & Hoppe, P. 2004, *Lunar Planet. Sci.*, 35, 1271
- Mostefaoui, S., Lugmair, G. W., & Hoppe, P. 2005, *ApJ*, 625, 271
- Nagahara, H. 1981, *Nature*, 292, 135
- Nakamoto, T., Hayashi, M. R., Kita, N. T., & Tachibana, S. 2005, *Lunar Planet. Sci.*, 36, 1256
- Nyquist, L. E., Bansal, B., Wiesmann, H., & Shih, C.-Y. 1994, *Meteoritics*, 29, 872
- Nyquist, L., Lindstrom, D., Shih, C.-Y., Wiesmann, H., Mittlefehldt, D., Wentworth, S., & Martinez, R. 2001, *Meteorit. Planet. Sci.*, 36, 911
- Nyquist, L. E., Reese, Y., Wiesmann, H., Shih, C.-Y., & Takeda, H. 2003, *Earth Planet. Sci. Lett.*, 214, 11
- Palme, H., Pack, A., Shelley, J. M. G., Burkhardt, C. 2004, *Lunar Planet. Sci.*, 35, 2023
- Papanastassiou, D. A., & Wasserburg, G. J. 1969, *Earth Planet. Sci. Lett.*, 5, 361
- Patterson, C. C. 1955, *Geochim. Cosmochim. Acta*, 7, 151
- Patterson, C. C. 1956, *Geochim. Cosmochim. Acta*, 10, 230
- Podosek, F. A., Zinner, E. K., MacPherson, G. J., Kundberg, L. L., Branon, J. C., & Fahey, A. J. 1991, *Geochim. Cosmochim. Acta*, 55, 1083
- Rambaldi, E. R., & Wasson, J. T. 1981, *Geochim. Cosmochim. Acta*, 45, 1001
- Rubin, A. E., Kallemeyn, G. W., Wasson, J. T., Clayton, R. N., Mayeda, T. K., Grady, M., Verchovsky, A. B., Eugster, O., & Lorenzetti, S. 2003, *Geochim. Cosmochim. Acta*, 67, 3283
- Russell, S. S., Srinivasan, G., Huss, G. R., Wasserburg, G. J., & MacPherson, G. J. 1996, *Science*, 273, 757
- Sheng, Y. J. 1992, Ph.D. thesis, Caltech, 271 pp.

- Sheng, Y. J., Hutcheon, I. D., & Wasserburg, G. J. 1991, *Geochim. Cosmochim. Acta*, 55, 581
- Sheng, Y. J., Hutcheon, I. D., & Wasserburg, G. J. 1992, *Geochim. Cosmochim. Acta*, 56, 2535
- Shukolyukov, A., & Lugmair, G. W. 1993a, *Science*, 259, 1138
- Shukolyukov, A., & Lugmair, G. W. 1993b, *Earth Planet. Sci. Lett.*, 119, 159
- Shukolyukov, A., & Lugmair, G. W. 1996, *Meteorit. Planet. Sci.*, 31 Suppl., A129
- Shukolyukov, A., Lugmair, G. W., & Bogdanovski, O. 2003, *Lunar Planet. Sci.*, 34, 1279
- Srinivasan, G., Ulyanov, A. A., & Goswami, J. N. 1994, *ApJ*, 431, L67
- Srinivasan, G., Huss, G. R., & Wasserburg, G. J. 2000, *Meteorit. Planet. Sci.*, 35, 1333
- Steiger, R. H., & Jäger, E. 1977, *Earth Planet. Sci. Lett.*, 36, 359
- Tachibana, S., & Huss, G. R. 2003, *ApJ*, 588, L41
- Tachibana, S., Nagahara, H., Mostefaoui, S., & Kita, N. T. 2003, *Meteorit. Planet. Sci.*, 38, 939
- Tachibana, S., Huss, G. R., Kita, N. T., Shimoda, H., & Morishita, Y. 2005, *Lunar Planet. Sci.*, 36, 1529
- Tatsumoto, M., Knight, R. J., & Allègre, C. J. 1973, *Science*, 180, 1279
- Tatsumoto, M., Unruh, D. M., & Desborough, G. A. 1976, *Geochim. Cosmochim. Acta*, 40, 617
- Taylor, D. J., McKeegan, K. D., Krot, A. N., & Hutcheon, I. D. 2004, *Meteorit. Planet. Sci.*, 39 Suppl., A104
- Taylor, D. J., McKeegan, K. D., & Krot, A. N. 2005, *Lunar Planet. Sci.*, 36, 2121
- Tilton, G. R. 1988a, in *Meteorites and the Early Solar System*, eds. J. F. Kerridge, & M. S. Matthews (Tucson: Univ. Arizona Press), 249
- Tilton, G. R. 1988b, in *Meteorites and the Early Solar System*, eds. J. F. Kerridge, & M. S. Matthews (Tucson: Univ. Arizona Press), 257
- Tomomura, S., Tachibana, S., Nagahara, H., Kita, N. T., & Morishita, Y. 2004, *Lunar Planet. Sci.*, 1555
- Wadhwa, M., & Russell, S. S. 2000, in *Protostars and Planet IV*, eds. V. Mannings, A. P. Boss, & S. S. Russell (Tucson: Univ. Arizona Press), 995
- Wadhwa, M., Amelin, Y., Bogdanovski, O., Shukolyukov, A., & Lugmair, G. W. 2005, *Lunar Planet. Sci.*, 36, 2126
- Weber, D., Zinner, E., & Bischoff, A. 1995, *Geochim. Cosmochim. Acta*, 59, 803
- Weidenschilling, S. J., Marzari, F., & Hood, L. L. 1998, *Science*, 279, 681
- Weinbruch, S., Palme, H., & Spettel, B. 2000, *Meteorit. Planet. Sci.* 35, 161
- Young, E. D., Simon, J. I., Galy, A., Russell, S. S., Tonui, E., & Lovera, O. 2005, *Science* 308, 223
- Yurimoto, H., & Wasson, J. T. 2003, *Geochim. Cosmochim. Acta*, 66, 4355
- Yurimoto, H., Koike, O., Nagahara, H., Morioka, M., & Nagasawa, H. 2000, *Lunar Planet. Sci.*, 31, 1593
- Zinner, E., & Göpel, C. 2002, *Meteorit. Planet. Sci.*, 37, 1001